6-28-2023

Developing and Testing Low-Cost Air Cleaners for Safer Spaces During Wildfires

Brett William Stinson
Portland State University

Developing and Testing Low-Cost Air Cleaners for Safer Spaces During Wildfires

by

Brett William Stinson

A thesis submitted in partial fulfillment of the
requirements for the degree of

Master of Science
in
Mechanical Engineering

Thesis Committee:
Elliott Gall, Chair
Alex Hunt
Erin Shortlidge

Portland State University
2023

Abstract

Air cleaning reduces indoor exposure to fine particulate matter ($PM_{2.5}$) during wildfire events.[1–3] However, resource and cost restraints may limit access to air cleaning during such an event, as both commercial devices and the high-rated MERV filters that homemade assemblies typically rely upon tend to be expensive and in short supply. With these barriers in mind, we sought to develop and evaluate the potential for air cleaners that use common household fabrics as filtration media. Evaluated designs use a box fan to move air across fabric filters; box fans are inexpensive and readily available to many households. Ultimately, this research aims to advance both fundamental understanding and practical considerations for recommending emergency-use air cleaning technologies.

Using mass balance principles to model a hypothetical indoor space during a wildfire, a target $PM_{2.5}$ clean air delivery rate (CADR)—or volumetric flowrate of clean air delivered by an air cleaner—for an effective do-it-yourself (DIY) device was predicted to be 127 m^3/h. Three distinct experimental methods were employed to determine if various configurations of the air cleaner met or exceeded this target. First, particle decay tests in two residential homes were conducted using incense combustion emissions as the challenge aerosol. A prototype air cleaner—which consisted of a box fan equipped with a cotton batting filter—yielded a $PM_{2.5}$ CADR of 177 m^3/h, 39% greater than the target. This CADR resulted in a net $PM_{2.5}$ removal effectiveness of >80% within 30 minutes of operation.

We then conducted laboratory testing of the device—again using incense combustion emissions as the challenge aerosol—independently characterizing air flowrates

and single-pass removal efficiencies to determine size-resolved, predicted CADRs. Five fabric filters (cotton batting, polyester, felt, flannel, and chiffon) were tested, as well as two popular, homemade air cleaning configurations with and without flowrate-increasing shrouds. Of the five fabrics tested, cotton batting yielded the highest predicted CADRs: at the highest fan speed setting with a single layer of fabric, average CADRs of 98, 80, and 192 m^3/h were realized at particle size ranges of 0.02–0.3, 0.3–1, and 1–2.5 µm, respectively.

Finally, particle decay testing in a large-scale chamber was conducted on the device with a cotton batting filter attached, including alternative configurations that featured a second filter and flowrate-increasing shroud. Across triplicate experiments with combustion emissions from pine needles local to Portland, Oregon as the challenge aerosol, the device with two layers of fabric and shroud yielded the highest average CADRs: 190, 158, and 243 m^3/h at particle size ranges of 0.02–0.3, 0.3–1, and 1–2.5 µm, respectively.

In an effort to directly compare results across laboratory and large-scale chamber experiments, an additional round of chamber testing was performed with a single cotton batting filter using the same box fan and challenge aerosol as the laboratory experiment (incense combustion emissions). The device yielded average CADRs that were 49%, 1%, and 6% higher than the corresponding laboratory experiment predicted CADRs, at particle size ranges of 0.02–0.3, 0.3–1, and 1–2.5 µm, respectively. While there was agreement between these experimental approaches in the two larger size bins, laboratory testing underpredicted CADRs in the 0.02–0.3 µm size range, a discrepancy that could be

explained by relative humidity and peak $PM_{2.5}$ injection concentration inconsistencies across experiments.

The three distinct approaches used here to determine CADRs yielded generally consistent results, demonstrating the fundamental scientific principles that govern active indoor air cleaning. While single-pass fabric removal efficiencies are generally low, large surface areas and high air flowrates make for an effective, low-cost air cleaning device, constructed of materials readily available to most during a wildfire event. There is limited data in the literature regarding the performance of DIY air cleaners, especially for the novel fabric-based designs developed as part of this work. These designs are simple, effective, and inexpensive, such that they represent a viable option for improving indoor air quality during a wildfire event.

Acknowledgements

This work was partially supported by an award from the U.S. Environmental Protection Agency's *Cleaner Indoor Air During Wildfires Challenge*.

Table of Contents

List of Tables

List of Figures

Section 1: Introduction

Though outdoor air quality has been steadily improving in the United States since the passing of the Clean Air Act in 1963,[4] the number of acres burned due to wildfires each year has grown significantly.[5,6] Wildfires pose a hazard to human health by increasing air pollutants—such as fine particulate matter ($PM_{2.5}$), or particles in air that are less than 2.5 µm in diameter—to levels that increase respiratory morbidity[7–9] and can exacerbate adverse cardiovascular effects,[10] especially in vulnerable populations such as children and the elderly.[11–14] While health agencies generally recommend sheltering indoors to reduce exposure to wildfire smoke, outdoor air (along with products of burning biomass, such as $PM_{2.5}$) infiltrates all buildings during a wildfire event.[15,16] While staying indoors may have some protective benefit during such an event (this will be explored further in *Section 2*), active air cleaning systems are also necessary, as they decrease indoor pollutant concentrations to levels that reduce the adverse health outcomes associated with exposures.

Indoor air cleaning interventions have been proven to reduce exposure to $PM_{2.5}$ during a wildfire event.[1–3] Efficacious air cleaners typically rely upon a fan to move air through a mechanical or fibrous media air filter in order to remove particles.[17] However, as we have seen in previous years—particularly during the Western U.S. wildfires of late summer 2020—traditional MERV and HEPA filters may be cost-prohibitive, in short supply, or in many cases, unavailable during such an occurrence. Thus, it is critical that new, low-cost solutions are developed to help those affected by degraded air quality. Access to these solutions will improve human health, quality of life, and in some cases,

prevent untimely death. With such cost and resource constraints in mind, we developed a prototype air cleaner that utilizes affordable, common household fabrics to create low-cost particle filters that can be attached to a box fan. This design allows for the creation of a large surface area of reusable filter, enabling the box fan to move high flowrates of air across the material.

In late 2020, the United States Environmental Protection Agency (U.S. EPA) began accepting proposals for their *Cleaner Indoor Air During Wildfires Challenge*,[18] which tasked researchers with developing a solution that reduces indoor $PM_{2.5}$ levels by 80% within an hour in a 14 m^2 room with 2.4 m ceilings, all while operating at less than 45 decibels and costing less than $100. As will be shown subsequently in *Section 4.1*, these criteria formed the basis of our initial targets while developing an impactful air cleaner.

In order to verify the general effectiveness of the device prior to submission, we conducted a field study. Particle decay testing was performed in two residential homes on the prototype with a cotton batting filter attached, using incense combustion emissions as the challenge aerosol. Results were promising, and thus two distinct experimental efforts were pursued with the goal of understanding the underlying physical phenomena that impact particle removal; these experimental efforts also created opportunities for maximizing the device's clean air delivery rate (CADR), or volumetric flowrate of clean air that an air cleaner is capable of distributing to an indoor space.

First, in a laboratory setting, we directly measured the air flowrate at three fan speeds through the device. We then measured the single-pass removal efficiency—or

efficiency of particle removal attained when a volume of air passed once through our experimental apparatus—of five selected fabrics (cotton batting, polyester, flannel, felt, and chiffon) and a MERV 13 filter, using incense combustion emissions as the challenge aerosol. These two metrics were combined to arrive at the air cleaner's predicted CADR.

Secondly, because cotton batting proved to be the most efficient fabric filter, we conducted particle decay testing in a large-scale chamber using combustion emissions from pine needles local to Portland, Oregon as the challenge aerosol. We tested alternative configurations of the device in an effort to increase its CADR, modifying it to include a second filter and flowrate-increasing shroud. To directly compare results across these two experimental setups, a round of chamber testing was performed on the device with a single cotton batting filter, using the same box fan and challenge aerosol (incense combustion emissions) as the laboratory testing described previously.

There is limited data in the literature regarding the performance of do-it-yourself (DIY) air cleaners, especially for the novel fabric-based designs developed as part of this work. Field, laboratory, and large-scale chamber results indicate that low-cost, fabric configurations can meaningfully reduce $PM_{2.5}$ levels in smaller zones of a home, such as bedrooms. Our design is simple, effective, and inexpensive, such that it represents a viable option for improving indoor air quality during a wildfire event.

Section 2: Background

2.1 Modeling an Indoor Space Using Mass Balance Principles

During a wildfire event, outdoor air inevitably enters indoor environments, bringing with it harmful pollutants released from burning biomass. In order to model indoor spaces as they interact with polluted air, mass conservation principles can be employed. *Equation 1* is a differential equation that leverages fundamental fluid dynamics concepts to parameterize source and loss mechanisms typical of an indoor space.

$$\frac{dC_i}{dt} = P\lambda C_o - \lambda C_i + \frac{S}{V} - LC_i \qquad \textit{(Eq. 1)}$$

where C_i is the indoor pollutant concentration (μg/m^3), t is time (h), P is the penetration factor (-), λ is the air exchange rate (h^{-1}), C_o is the outdoor pollutant concentration (μg/m^3), S is the indoor pollutant source term (μg/h), V is the volume of the indoor space (m^3), and L is the indoor pollutant loss rate (h^{-1}).

Using a control volume to model the indoor space (*Figure 1*), elements of the building envelope (walls, floor, roof, etc.) represent the control surface that air crosses as it enters from outside and exits from inside. A few key assumptions must be made with regard to the control volume: 1) it is fixed in space through time, 2) the density of the fluid within it is constant, 3) the air present within it is well-mixed, 4) the mass within it can only be transformed (not created or destroyed), and 5) source and loss coefficients are constant. Because the volume of the modeled space and density of the fluid within it are assumed to be constant, the air flowrate entering and exiting the control volume is equal. Because the space is assumed to be well-mixed, the pollutant of interest's concentration is equal to its concentration as it leaves the space.

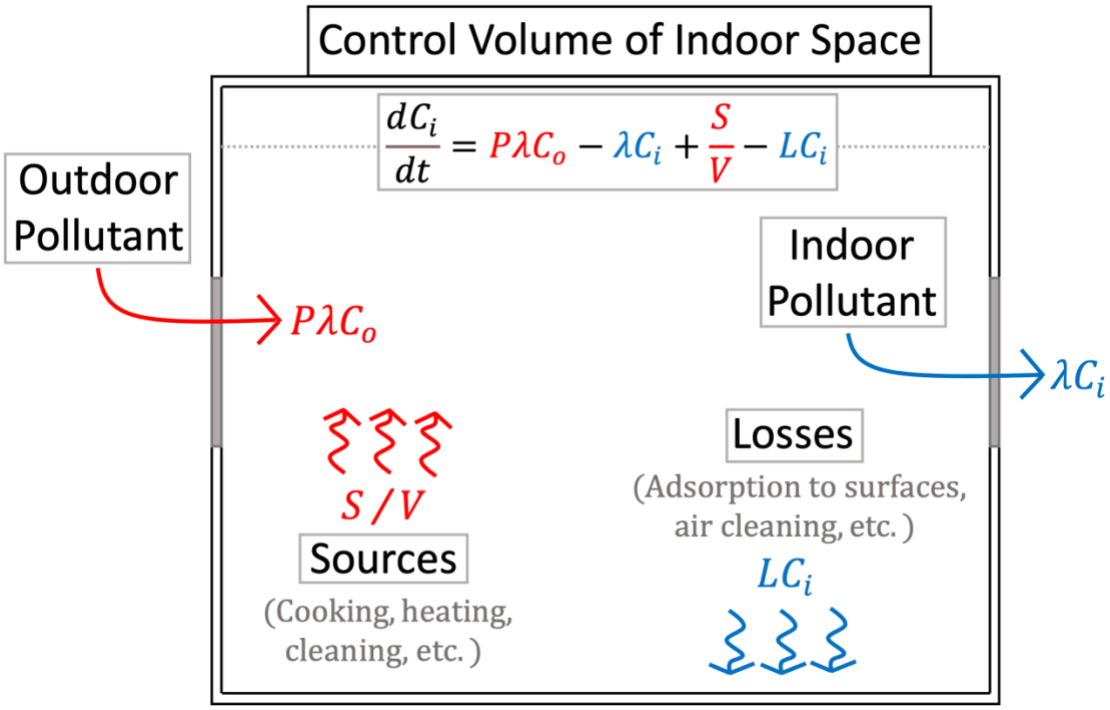

Figure 1: Control volume of an indoor space modeled using *Equation* 1, a dynamic mass balance

The left hand side of *Equation 1* represents the time-varying accumulation of a pollutant within the indoor space. Terms on the right hand side of *Equation 1* are either inputs to the control volume, increasing indoor pollutant concentrations by entering from outside or being emitted from the space itself ($P\lambda C_o$ and $\frac{S}{V}$, respectively), or outputs from the control volume, decreasing indoor pollutant concentrations by exiting the space to the outside or being removed through indoor mechanisms (λC_i and LC_i, respectively).

Examining each of the input terms in greater detail, beginning with $P\lambda C_o$, C_o represents the outdoor concentration of the pollutant of interest. λ is the air exchange rate, or the number of times the air in a space is replaced completely by outdoor air, typically reported in units of inverse hours; the inverse of the air exchange rate is air detention time, or the amount of time a volume of air spends inside of a space. Adequate air exchange is a

critical component of maintaining satisfactory indoor air quality,[19] and is typically achieved through three mechanisms: 1) mechanical ventilation, where an air handler draws outdoor air into a building and recirculates indoor air, 2) natural ventilation, where large openings in the building envelope are intentionally designed to facilitate outdoor airflow, and 3) infiltration, where uncontrolled air enters the building via deficiencies in its envelope such as cracks and gaps. Because infiltration through a space is uncontrolled, it is accounted for separately with *P*, the penetration factor, which is defined as the fraction of an air pollutant that crosses the building envelope and enters the indoor space via infiltration. Residential buildings tend to rely on infiltration for air exchange; an air exchange rate of 0.5 h^{-1} and a $PM_{2.5}$ penetration factor of 0.7 is typical for single-family homes.[20,21] The second input term, $\frac{S}{V}$, describes emissions from indoors (*S*) divided by the space's volume (*V*). While there exists a myriad of harmful pollution sources present indoors at any given time, some of the more prevalent are fuel-burning combustion appliances (predominantly those used for cooking[22,23] and heating[24]), cleaning products,[25] tobacco smoke,[26] and building materials.[27,28]

Examining each of the output terms in greater detail, beginning with λC_i, C_i represents the indoor concentration of the pollutant of interest and λ is the air exchange rate, which was defined previously. The second output term, LC_i, accounts for losses to the indoor space, which can occur due to a number of processes, the two most prevalent being removal to surfaces (such as walls, floors, and furniture; the indoor $PM_{2.5}$ deposition loss rate (L_{dep}) typical of a residential building is 0.4 h^{-1})[29] and air cleaning, the intentional removal of air pollutants from a space.

2.2 Air Cleaning as a Removal Mechanism

While several active air cleaning technologies exist, including those that rely on processes that employ sorbents, photocatalytic oxidation, ultraviolet germicidal energy, the production of ozone, etc.,[30] the most common technology (and the one explored throughout this work) is air cleaning via mechanical filtration. This method relies on fibers or membranes present on media of a porous structure to separate particles from air. The portable air cleaners examined as part of this study are considered to be open-path, meaning they recirculate air inside of the space (as opposed to closed-path air cleaning which cleans air being supplied from outside). An active recirculating air cleaner is a loss mechanism that can be modeled independently using *Equation 2*.

$$L_{AC} = \frac{Q_{AC}}{V}\eta \qquad \textit{(Eq. 2)}$$

where L_{AC} is the air cleaner's loss rate ($h^{=1}$), Q_{AC} is the volumetric air flowrate entering and exiting the air cleaner (m^3/h), V is the volume of the indoor space (m^3), and η is air cleaner's removal efficiency (-).

To summarize the process, a pollutant enters an air cleaner at a volumetric flowrate that is normalized by the volume of the space (Q_{AC}/V) and is removed with some amount of efficiency (η). Loss mechanisms are presented in *Equation 1* with negative signs preceding them, indicating that some concentration of the pollutant of interest is being removed from the space due to the air cleaner's presence. Thus, the product of Q_{AC}/V and η is known as the loss rate of an air cleaner and can be multiplied by a pollutant's concentration to quantify how much of it is being removed.

A useful metric for determining the effectiveness of an air cleaner independently from the space it occupies is its CADR,[31] or volumetric flowrate of clean air delivered by a device, typically reported in units of m^3/h or ft^3/min. Deconstructing *Equation 2*, the product of the two variables specific to the device itself, Q_{AC} and η, is the CADR (*Equation 3*).

$$CADR = Q_{AC}\eta \qquad \textit{(Eq. 3)}$$

where all terms have been defined previously.

2.3 Characterizing the Effectiveness of an Air Cleaner

ANSI/AHAM AC-1[31] establishes a uniform, repeatable procedure for testing the particulate matter CADR of air cleaning devices. To summarize the test method briefly, an air cleaner is placed in an airtight (λ <0.03 h^{-1}), 29 m^3 environmentally controlled chamber (held at 23 ± 3 °C, 40 ± 5% relative humidity) and challenged by three aerosols that produce particles of different diameter size ranges: tobacco smoke (0.09–1 µm), dust (0.5–3 µm), and mulberry pollen (5–10 µm). Because dust and pollen are relatively easy to remove from a space, a device's smoke CADR is its most meaningful efficacy metric—if an air cleaner is effective at removing smoke, it is generally the case that it will also be effective at removing dust and pollen, though the reverse is not necessarily true. The procedure begins by injecting the chosen challenge aerosol into the test chamber while the air cleaner is non-operational, aiming for a peak particle concentration of 24,000–35,000 particles/cm^3 during smoke injections. Particles are allowed to decay naturally until baseline concentrations are returned to (<20 particles/cm^3), which accounts for background particulate matter losses to the chamber. The challenge aerosol is then injected again and

allowed to decay for 20 minutes while the device is operational. Multiplying the difference between the loss terms when the air cleaner is non-operational versus operational (which are determined using a regression analysis on particle decay curves, a process described in greater detail in *Section 3.3*) by the volume of the chamber results in the device's CADR.

While the ANSI-AHAM AC-1 test method served as inspiration for the field and large-scale chamber portions of this study, there are a few key differences in our approach (apart from the volume of the chamber and its environmental conditions, described in *Section 3.2.4*). First, the ANSI-AHAM AC-1 method employs a batch process, where all losses inside of a space are lumped into a single term. This assumes that the chamber is airtight ($\lambda = 0$)—that is, no losses are occurring due to air exchange between the chamber and its surroundings—which may not be the case, especially during a field study. To account for potential losses due to air exchange, an inert, gaseous tracer (CO_2 for these experiments) was injected simultaneously with the chosen challenge aerosol and allowed to decay alongside it. Using a regression analysis on the CO_2 decay period, an air exchange rate corresponding to the length of the experiment could be calculated and subtracted from particle loss rates. Secondly, because the focus of this study is affordable air cleaning solutions during wildfire events, we opted to combust pine needles local to Portland, Oregon as the challenge aerosol during chamber testing, rather than tobacco smoke. While the combustion of tobacco and biomass both generate smoke, different compounds are produced; the aim was to simulate wildfire conditions as closely as possible.

2.4 Literature Review

A number of studies have explored the importance of active air cleaning interventions during wildfire events. During the Western U.S. wildfires of 2020, Xiang et al. 2021[32] monitored $PM_{2.5}$ levels inside of seven Seattle, WA residences, building mass balance models to determine the removal efficiency of a commercial, HEPA filter-based portable air cleaner. Using nearby government air quality monitoring stations to track outdoor levels, they found that the use of air cleaning interventions decreased $PM_{2.5}$ concentrations by 48%–78%. Also conducting a study in Seattle, WA during the 2020 wildfire season, He et al. 2022[33] found that in a set of seven homes equipped with HEPA-rated air cleaners, a 50%–77% reduction in $PM_{2.5}$ concentrations was realized. During the 2018 wildfire season, Stauffer et al. 2020[2] measured $PM_{2.5}$ concentrations over an eight day period in two identical Pacific Northwest offices, one containing a HEPA-rated portable air cleaner. They found that indoor $PM_{2.5}$ concentrations were reduced by 73% during occupied working hours (8:00–16:00) and 92% during non-working hours (22:00–6:00). Henderson et al. 2005[3] employed portable electrostatic precipitating air cleaners in four Colorado homes (two with air cleaners present and two without) during four fire events, monitoring $PM_{2.5}$ levels indoors and outdoors. $PM_{2.5}$ concentrations were decreased by 63%–88% in residences with air cleaners versus those without.

While the effectiveness of commercial portable air cleaners during wildfire events has been established, low-cost, DIY alternatives have become prevalent in recent years. Holder et al. 2022[1] studied several of these alternatives under simulated wildfire conditions (using burning pine needles as the challenge aerosol), focusing primarily on various

configurations of a MERV-rated furnace filter affixed to a box fan. They found that taping a MERV 13 filter to a box fan and operating it on its highest setting resulted in a CADR of 189 ± 2 m^3/h, while the addition of a cardboard shroud increased this CADR by ~40% to 265 ± 6 m^3/h. Arranging four of the same filters into a Corsi-Rosenthal box design yielded a CADR of 681 ± 52 m^3/h. May et al. 2021[34] evaluated the effectiveness of a similar low-cost configuration (a MERV 13 filter affixed to a box fan with tape) during the Western U.S. wildfires of 2020, operating the air cleaner in two Seattle, WA rooms while outdoor $PM_{2.5}$ levels were recorded at 127 ± 9 µg/m^3. Once the device was activated, $PM_{2.5}$ concentrations dropped by 56% after 90 minutes of operation in the first room and 99% in less than 60 minutes in the second room. Using NaCl as the challenge aerosol, Dal Porto et al. 2022[35] explored the effectiveness of a Corsi-Rosenthal box with five MERV 13 filters arranged to form a cube. At the box fan's highest speed setting, they measured $PM_{2.5}$ CADRs (recording in the 0.5–20 µm range) exceeding 1300 m^3/h in a classroom and home office setting.

There is limited data in the literature regarding the effectiveness of low-cost, DIY air cleaning solutions during wildfire events, especially those that do not rely upon high-rated MERV and HEPA filters, which may be in short supply during an emergency scenario. While a portion of this study found us characterizing predicted CADRs for configurations similar to the DIY air cleaners mentioned above, our primary goal was to assess the effectiveness of novel, fabric-based devices, constructed of materials likely accessible to most during a wildfire event.

Section 3: Methods and Materials

The aim of this study was to evaluate low-cost air cleaner designs that employ a box fan to move air across a variety of particle filtration materials. After modeling an effective air cleaner during a wildfire event to determine a target CADR (*Section 4.1*), several phases of experimental measurements were conducted in support of this objective. *Section 3.2.1* describes what will henceforth be known as "field testing", where particle injection and decay was carried out under real-world environmental conditions, *Sections 3.2.2* and *3.2.3* describe what will henceforth be known as "laboratory testing", where air flowrates and single-pass removal efficiencies were characterized separately and combined to determine predicted CADRs (as shown previously in *Section 2.2*), and *Section 3.2.4* describes what will henceforth be known as "large-scale chamber testing", where a method that relies on particle injection and decay was employed under controlled conditions within a large chamber. Because laboratory and large-scale chamber testing utilized highly controlled, entirely independent approaches to determine the prototyped device's CADR, we took advantage of the opportunity to compare results across experimental efforts. The methods described in *Section 3.2.4* were employed to test a configuration of the device that was analyzed during laboratory testing, using the same fabric, box fan, and challenge aerosol. Results of the aforementioned experiments can be found in *Sections 4.2–4.4*, while a comparison between laboratory and chamber experiments is discussed in *Section 4.5*

3.1 Low-Cost Air Cleaner Materials

We developed a prototype air cleaner and modified it throughout the described experiments to improve its CADR across each phase of the project. During field testing, a

1.8 m long “windsock”, cut from a roll of cotton batting fabric purchased from JOANN Fabric and Crafts, was sewn to be open at both ends and affixed to a 53 x 54 x 11 cm Holmes box fan (Model HBF2010A-WM) with either a ratchet strap or zip ties, depending on the location of the field study (*Figure 2a*). The side of the windsock that was not attached to the fan was folded neatly three times from the bottom and tied 8 cm from its end with two double-looped rubber bands.

During laboratory testing, five fabrics (cotton batting, polyester, flannel, felt, and chiffon, all purchased from JOANN Fabric and Crafts) were sewn into 1–1.8 m long windsocks (the length depending on the fabric) and affixed to a 53 x 57 x 13 cm Comfort Zone box fan (Model CZ200A) with zip ties (*Figure 2b*). Two additional device configurations were tested for comparison during this phase: a single 51 x 51 x 5 cm MERV 13 filter and a modified Corsi-Rosenthal Box (which consisted of 4 MERV 13 filters arranged to form a cube), both affixed to the same box fan with duct tape. Small swatches of each of the fabrics and a MERV 13 filter were cut and attached to filter holders with two, double-looped rubber bands during single-pass removal efficiency testing.

During full-scale chamber testing, two new cotton batting filters were sewn to fit snugly around a 53 x 61 x 18 cm Air King box fan (Model 9723). A flowrate-increasing shroud (*Figure 2c*) was cut from cardboard and attached to the outtake side of the box fan during select experiments. *Figure 2* presents configurations of the prototype air cleaner during each phase of testing.

Figure 2: Image of low-cost air cleaner with a) cotton batting filter attached during the field testing, *b)* chiffon filter attached during laboratory testing, and *c)* cardboard shroud affixed during large-scale chamber testing

3.2 Experimental Design

3.2.1 Field Testing

Field testing was carried out a total of four times using the prototype configuration discussed in *Section 3.1*: twice at location 1, in the bedroom of a home constructed in 1890 in Portland, OR, and twice at location 2, in the bedroom of a home constructed in 1920 in Rhododendron, OR. Location 1 is a 3 x 3.7 x 3 m, 34 m^3 carpeted bedroom with walls and ceiling constructed of painted drywall. There are three shared walls, one wall to the exterior, and one window. The furniture included a raised, full-sized mattress, corner couch, desk, two computer monitors, and five pieces of unfinished wood furniture. The first and second trials of the experiment at location 1 were carried out on 05/01/21 and 05/02/21, respectively. Location 2 is a 2.6 x 2.7 x 2.4 m, 16.5 m^3 office with wood floors, and walls and ceiling constructed of wood paneling. There are two shared walls: one between the office and a bedroom, the other with a door that led to a large living area with high ceilings; three small windows lined the opposite, exterior-facing walls. The furniture included a desk, office chair, couch, electronic keyboard, computer monitor, printer, two small suitcases, filing cabinet, and a rug placed in the center of the room. The

first and second trials of the experiment at location 2 were carried out on 04/22/21 and 04/23/21, respectively. *Figure A.1* in the Appendix presents images of the experimental setup at both locations.

To monitor $PM_{2.5}$ levels, a laser particle counter (Dylos DC1700) was employed, operating continuously in intervals of 1 minute. Because this particle counter reports $PM_{2.5}$ concentrations in units that are distinct from more common metrics (such as $\mu g/m^3$ or particles/cm^3), conversions were made from particles/ft^3/100 to $\mu g/m^3$ via regression equations present in Steinle et al. 2015.[36] To monitor CO_2 levels, a battery-powered CO_2 logger (Onset HOBO MX1102) was employed, operating continuously and reporting in units of ppm in intervals of 1 minute. The CO_2 logger also recorded temperature, relative humidity, and dew point. To elevate indoor $PM_{2.5}$ levels, Mainichi-Koh sandalwood incense was burned. A second box fan was present in each location to ensure proper mixing.

The room's air exchange rate was found before each experiment by elevating CO_2 concentrations above 1000 ppm through excessive breathing and talking with the windows and doors closed. Once 1000 ppm was reached, the space was vacated and the CO_2 concentration was allowed to decay for approximately 100 minutes. An outdoor CO_2 concentration of 420 ppm was assumed for air exchange rate calculations—a conservatively low estimate based on average outdoor CO_2 levels in and near Portland, OR, U.S.A.[37]

Each trial began by recording background $PM_{2.5}$ measurements for a minimum of ten minutes inside of the sealed room. The mixing fan was then engaged, and three sticks

of incense were lit simultaneously and placed upright into a small jar containing sand for 1–2 minutes. Upon extinguishing the incense in the same jar of sand, the mixing fan was immediately turned off and the experimenter left the room—particles were allowed to decay for 30–45 minutes. The air cleaner was present in the room but remained non-operational for this portion of the experiment, which allowed us to account for background losses of $PM_{2.5}$ to the room itself. Between experiments, windows and doors were opened, the mixing fan was turned on, and the room was flushed out until $PM_{2.5}$ levels returned to previous background concentrations—this process took between 15 and 30 minutes. Once this occurred, the doors and windows were closed and the room was vacated for 30 minutes, allowing for $PM_{2.5}$ concentrations to return to steady-state. The injection process was then repeated, but with the air cleaner operating. The air cleaner remained engaged until particle concentrations returned to steady-state levels for a minimum of ten minutes. The order in which experiments were carried out (having the air cleaner off versus having it on) was varied randomly.

3.2.2 Laboratory Testing: Air Flowrates

In order to measure air flowrates through the various air cleaners, a ducting system was constructed in the laboratory; a 0.6 x 0.6 m, 1.5 m long section of galvanized steel ducting was affixed to a 0.6 x 0.6 m, 1.7 m long section of cardboard ducting with foil duct tape (*Figure 3*). On the metal side, the air cleaner assembly was placed near the intake (*Figure 3*, right side of duct); gaps were closed with cardboard that was sealed with foil tape. A hot wire anemometer (TSI Alnor CompuFlow, Model 8585) was used to inspect for airflows around seals, consistently measuring <0.01 m/s. On the outlet side of the

makeshift duct (*Figure 3*, left side of duct), a piece of cardboard with a 250 mm diameter hole cut through its center was attached with duct tape; this allowed for connection via flex ducting to a calibrated fan (Energy Conservatory Minneapolis Duct Blaster). The flex ducting was sealed to the duct blaster fan and included a flow conditioner secured to its outer edge, which was equipped with the appropriate duct blaster ring, chosen based on its airflow range. A variable fan speed controller was used to adjust fan speed and a pressure gauge (Energy Conservatory, DG-700) was attached to the duct blaster fan via three pieces of 25 mm diameter tubing.

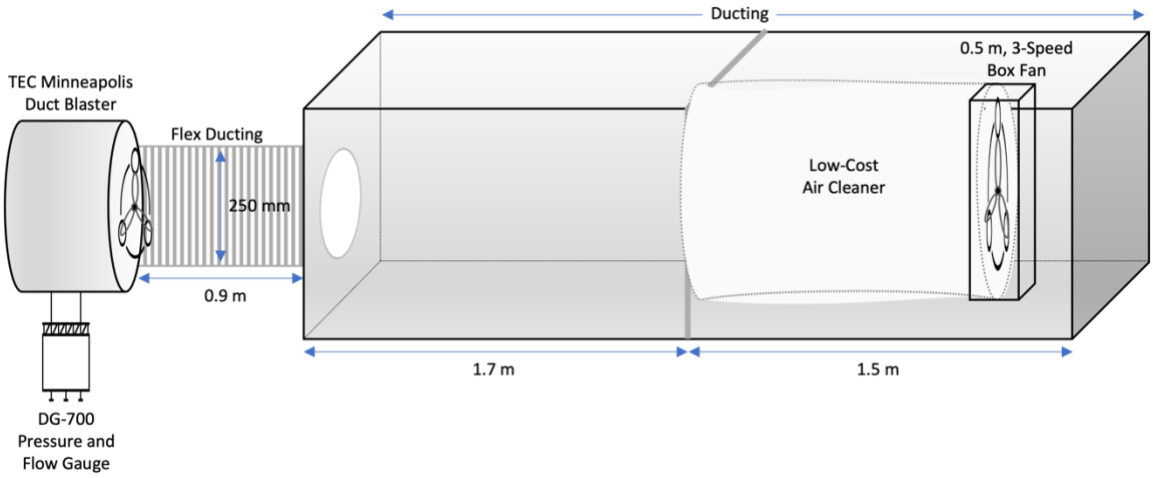

Figure 3: Schematic of air flowrate testing apparatus

Prior studies show particle removal efficiency varies as a function of face velocity,[38] or the airspeed across the material being tested, and therefore this parameter was necessary to inform subsequent single-pass removal efficiency experiments (See *Section 3.2.3*). Filter face velocities are typically calculated from the continuity equation using a measured flowrate and projected surface area of filter. The face velocity surface area of the low-cost air cleaner was estimated as the summation of the area of a cylinder (main body) and cone (end). To measure flowrates, the pressure matching method[39] was employed

within the section of ducting for each configuration of the air cleaner. Briefly, this method allowed total system airflow to be determined by increasing the speed of the calibrated fan until static pressure in the system with just the air cleaner operating was matched.

The test matrix consisted of eight configurations, run at three fan speeds each (low, medium, and high): the box fan with five different fabrics affixed to it (cotton batting, polyester, flannel, felt, and chiffon), the box fan with a single MERV 13 filter attached, the modified Corsi-Rosenthal Box, and the fan itself, as a control. The configurations with MERV 13 filters were tested both with and without a flow-enhancing shroud; a hole approximately equal to the diameter of the fan blades was cut into a 0.5 x 0.5 m piece of cardboard and affixed to the outlet side of the box fan. At each fan speed, flowrates were continuously averaged within the ducting over one minute three times, and then the average of the three trials was taken. Between each trial, the air cleaner and duct blaster fan were powered off for a minimum of thirty seconds.

3.2.3 Laboratory Testing: Single-Pass Removal Efficiencies

In order to directly measure the single-pass removal efficiency of particles across samples (the five chosen fabrics and MERV 13 filter), a bench-scale testing apparatus was constructed (*Figure 4*). A vacuum pump (KNF Neuberger 12V pump, Model NMP830KNDC) was used to draw air through the apparatus, which consisted of a primary flow calibrator (Sensidyne Gilibrator 2), used to measure flowrates, a particle counter (TSI, Model 3330), which measured particles from 0.3 to 10 µm in 16 adjustable size channels in one second intervals, and a condensation particle counter (TSI, Model 8525), which measured total particle counts from 0.02 to 1 µm in one second intervals. Duplicates of

three filter holders were constructed at diameters of 20-, 47-, and 100-mm. Conductive tubing (3/8" OD, Bev-A-Line), cut at the minimum length possible, was utilized to reduce particle deposition to tubing walls.

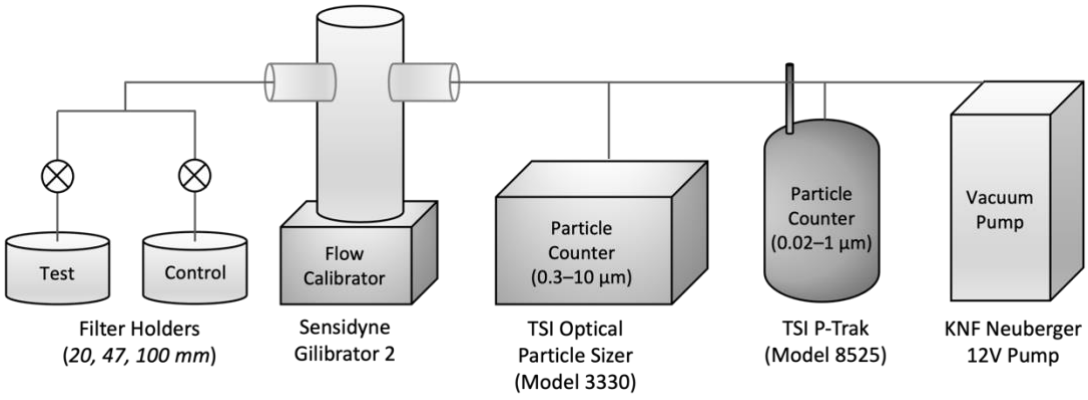

Figure 4: Schematic of single-pass removal efficiency testing apparatus

As previously stated, our aim was to conduct bench-scale removal efficiency testing at face velocities representative of the full-scale device. Air flowrate results from the pressure matching test (*Section 3.2.2*) were used to calculate the face velocity of the air cleaner (air flowrate (m^3/h) divided by the surface area of the fabric (m^2)). The diameter of filter holder during single-pass removal efficiency testing necessary to match this face velocity was back-calculated using total flowrates through the apparatus shown in *Figure 4*; diameters ranged from 24–108 mm. This range informed the selection of filter holders for testing (20-, 47-, and 100-mm).

Air flowrates through the system were held constant at 4 L/min; they were measured using the primary flow calibrator, which was removed from the apparatus prior to particle testing. Small samples of each of the five fabrics and the MERV 13 filter were cut and secured with two, double-looped rubber bands to the fabric holder used. This sample and a duplicate filter holder with no sample attached were exposed to simulated

wildfire particulate matter conditions, achieved with the burning of incense (Indo Lao Shan Sandalwood Incense Powder) via a countertop hot plate (Elite Gourmet ESB-301BF). Particulate matter concentrations were elevated to a maximum of 3000 particles/cm^3 in the 0.3 to 10 µm range (the detection limit of the Model 3330 particle counter) inside of a 0.6 x 0.6 m, 1.5 m long section of well-sealed galvanized steel ducting. A manual switching valve (via two ball valves placed downstream of each filter holder) allowed for alternation of sampling between the control (filter holder without filter) and test (filter holder with filter) in 150 second intervals for 15 minutes. Each fabric/filter size combination was tested in duplicate and averaged.

3.2.4 Large-Scale Chamber Testing

Large-scale chamber testing was conducted in a 21 m^3 stainless steel enclosure. Two three-speed desk fans (Vornado, Model CR1-0120-06) were placed in opposite corners of the chamber and operated at their highest setting to achieve well-mixed conditions; adequate mixing was confirmed via multi-point CO_2 tracer tests. The air cleaner was placed atop a 0.75 m table against the back center wall of the chamber. The TSI Model 3330 and Model 8525 particle counters were again used to measure concentrations in the 0.02–1 µm and 0.3–10 µm ranges, respectively; a manual switching valve allowed for sampling inside and outside of the chamber. For the challenge aerosol, 0.25 g of pine needles local to the region (Portland, Oregon) were burnt via a food smoking gun (Breville, Model BSM600SIL) for approximately six seconds. In order to calculate the air exchange rate of the chamber, CO_2 was injected at the same time as the challenge aerosol. CO_2 inside

and outside of the chamber was measured by battery-powered loggers (Onset HOBO MX1102)—these devices also measured temperature and relative humidity.

Because the cotton batting fabric filter yielded the highest predicted CADR during laboratory testing, it was chosen for further analysis in the large-scale chamber. In addition to testing the device with a single layer of fabric attached, it was also tested with a second layer of cotton batting fabric, which we predicted would increase removal efficiency, and a second layer of cotton fabric paired with an air flowrate-increasing shroud, which we predicted would increase flowrate. During all trials the device was operated at its highest fan speed setting.

Each trial began by taking background particle concentration and CO_2 measurements for five minutes outside and then ten minutes inside of the sealed chamber. The challenge aerosol and CO_2 were then injected and allowed to decay for 30 minutes. The air cleaner was present in the chamber but remained non-operational for this portion of the experiment, which allowed us to account for background $PM_{2.5}$ losses to the chamber itself. After 30 minutes, the chamber's ventilation system was engaged until particle and CO_2 concentrations returned to near-background levels. The chamber ventilation system was turned off and the injection process was then repeated, but with the air cleaner operating. The air cleaner remained engaged until particle concentrations returned to steady-state levels for a minimum of ten minutes.

3.3 Calculations

3.3.1 Field Testing

For field testing, an approach often employed to evaluate the effectiveness of an air cleaner (commonly called the "pull-down" method) was used.[40] Using *Equation 4*, which describes the time-varying concentration of $PM_{2.5}$ in each of the locations, a linear regression was performed for portions of the experiment where the air cleaner was non-operational, and again when it was operational, in order to determine total particle loss rates ($\lambda + \beta$) as the regression coefficient. The room's air exchange rate (λ), determined using a similar regression method with CO_2 concentrations (where C_{bg} = 420 ppm, the assumed outdoor CO_2 concentration[37]), was subtracted from this value to arrive at particle loss rate constants.

$$-ln\frac{C_{i,t} - C_{bg}}{C_{i,t=0} - C_{bg}} = (\lambda + \beta)t \qquad \textit{(Eq. 4)}$$

where $C_{i,t}$ is the particle concentration at time t (particles/cm^3), $C_{i,t=0}$ is the particle concentration at time $t=0$ (particles/cm^3), C_{bg} is the average background particle concentration measured during steady-state conditions (particles/cm^3), and ($\lambda + \beta$) is the total particle loss rate (h^{-1}).

The difference between particle loss rate constants when the air cleaner was on versus off was multiplied by the room's volume to arrive at the air cleaner's CADR (*Equation 5*).

$$CADR = \left(\left[(\lambda + \beta) - \lambda\right]_{on} - \left[(\lambda + \beta) - \lambda\right]_{off}\right]) \cdot V \qquad \textit{(Eq. 5)}$$

where V is the volume of the space (m^3), and all other terms are defined previously. The subscripts *on* and *off* represent periods where the air cleaner was operational and non-operational, respectively.

In order to find net log and net percentage reductions during field testing, *Equations 6* and *7* were used.

$$Net\ Log\ Reduction = \left[-log_{10}\left(\frac{C_{i,f}}{C_{i,t=0}}\right)\right]_{on} - \left[-log_{10}\left(\frac{C_{i,f}}{C_{i,t=0}}\right)\right]_{off} \quad \textit{(Eq. 6)}$$

$$Net\ \%\ Reduction = \left(1 - 10^{-(Net\ Log\ Reduction)}\right) \cdot 100 \quad \textit{(Eq. 7)}$$

where $C_{i,f}$ is the final $PM_{2.5}$ concentration and $C_{i,t=0}$ is the initial $PM_{2.5}$ concentration after a period of injection. The subscripts *on* and *off* represent periods where the air cleaner was operational and non-operational, respectively.

3.3.2 Laboratory Testing

For laboratory testing, predicted CADRs for the device were calculated using *Equation 3* in *Section 2.2*. Using the method described in *Section 3.2.2*, air flowrates at three fan speeds were measured directly (Q_{AC} from *Equation 3*) and removal efficiencies at each filter holder size were calculated using *Equation 8*:

$$\eta = \frac{C_{ambient} - C_{fabric}}{C_{ambient}} \quad \textit{(Eq. 8)}$$

where η is the single-pass removal efficiency of the fabric (%), $C_{ambient}$ is the ambient particle concentration (particles/cm^3) measured via the control filter holder, and C_{fabric} is the particle concentration downstream the filter (particles/cm^3) measured via the test filter holder.

3.3.3 Large-Scale Chamber Testing

For large-scale chamber testing, the "pull-down" method was again employed,[40] using the same methodology described in *Section 3.3.1*. For particles, the C_{bg} term present in *Equation 4* was determined by averaging steady-state concentrations inside of the

chamber. For periods when the air cleaner was off, this averaging occurred just before injection, while for periods when the air cleaner was on, averaging occurred once particle concentrations returned to steady-state levels. For CO_2, the C_{bg} term present in *Equation 4* was determined by averaging steady-state concentrations outside of the chamber just before both injections. *Equation 5* was again used to calculate CADRs.

Section 4: Results and Discussion

4.1 Target CADR Mass Balance Modeling

As stated in *Section 1*, the initial prototype was constructed in accordance with the requirements of the U.S. EPA's *Cleaner Indoor Air During Wildfires Challenge*.[18] Challenge requirements dictated that for an air cleaning solution to be considered successful, it must achieve greater than an 80% reduction of $PM_{2.5}$ concentration in one hour versus the $PM_{2.5}$ concentration in the same room without the air cleaner present. For the dimensions of the room given (14 m^2 floor area with a height of 2.4 m) and an outdoor $PM_{2.5}$ concentration of 165 $\mu g/m^3$ (which was determined by averaging the minimum (30 $\mu g/m^3$) and maximum (300 $\mu g/m^3$) concentrations given as a range of realistic wildfire $PM_{2.5}$ levels), typical residential conditions, as stated in *Section 2.1*, were assumed. *Equation 9* is the solution to *Equation 1* in *Section 2.1*, a differential equation describing the time-varying $PM_{2.5}$ concentration in the hypothetical space when accounting for air exchange, removal to background, and removal to the air cleaner, the three loss mechanisms present in *Equation 10*.

$$C_{i,t} = \left(P\frac{\lambda}{\alpha}C_o + \frac{S}{\alpha V}\right)(1 - e^{-\alpha t}) + C_{i,t=0}e^{-\alpha t} \qquad \textit{(Eq. 9)}$$

$$\alpha = \lambda + \frac{Q_{AC}\eta}{V} + L \qquad \textit{(Eq. 10)}$$

where all terms are defined previously in *Sections 2.1*, *2.2*, and *3.3.1*.

Figure 5 presents the results of indoor $PM_{2.5}$ concentration (*Equations 9* and *10*) versus time for the given conditions. In the hypothetical indoor space, absent air-cleaning, the $PM_{2.5}$ concentration will reach steady-state at approximately 64 $\mu g/m^3$ (*Figure 5*, red line). If an air cleaner is added to the room (*Figure 5*, blue line) with an initial condition of

64 µg/m^3, a dynamic mass balance using the same inputs shows that a CADR of 127 m^3/h results in an 80% reduction of $PM_{2.5}$ in one hour. Thus, a minimum CADR of 127 m^3/h was targeted.

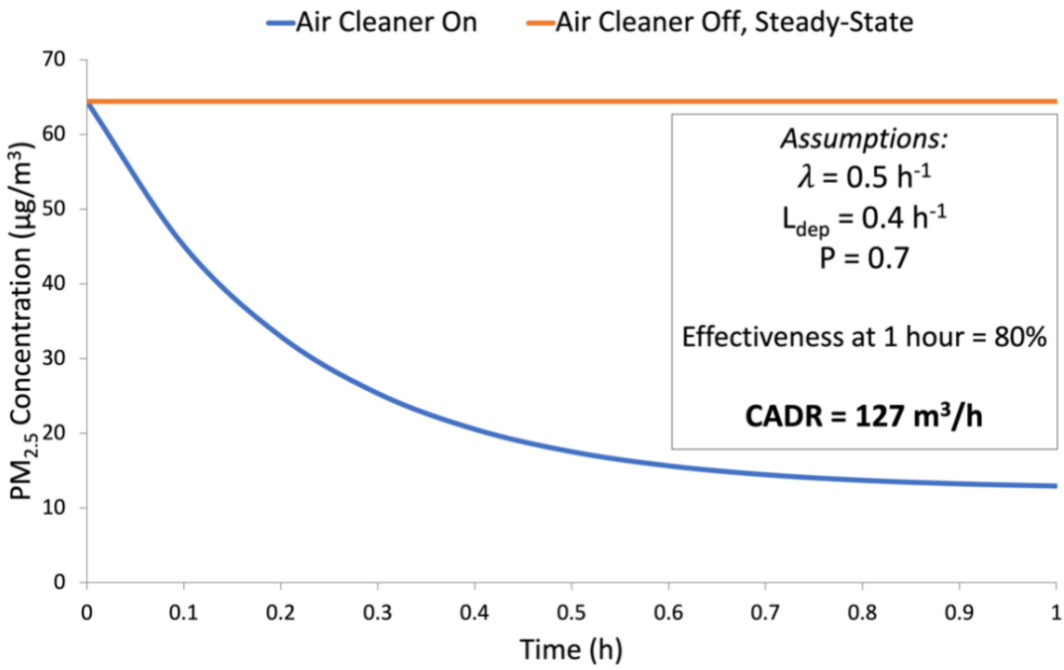

Figure 5: Plot of $PM_{2.5}$ concentration vs. time in the hypothetical space; assumptions were made in compliance with EPA challenge criteria

4.2 Field Testing

Field testing of the device with a cotton batting filter attached was carried out in two residential homes. Air exchange rates at locations 1 and 2 were found to be 0.77 h^{-1} and 0.84 h^{-1}, respectively. These are slightly higher than the average air exchange rate (0.5 h^{-1}) typical of residential buildings.[20] *Figure A.2* in the Appendix presents the regression analysis used to arrive at air exchange rates.

Figure 6a displays a sample plot of $PM_{2.5}$ concentration vs. time for the air cleaner and background tests at location 1 on 05/02/21. *Figure 6b* displays the linear regression for both tests, the corresponding slopes (particle loss rate constants), and the resulting CADR

calculation during the same experiment. As stated in *Section 4.1*, a CADR of 127 m^3/h was targeted. The air cleaner proved to be quite effective, yielding a CADR well above this metric for each experiment at both locations, delivering its most impressive results (211 m^3/h) on 05/02/21, shown below in *Figure 6b*. In all cases, the air cleaner began working immediately, yielding an average net $PM_{2.5}$ reduction of 84% after 30 minutes of operation following peak concentrations. Across four replicate experiments in two different bedrooms, the average CADR was 177 ± 24 m^3/h (avg. ± std. dev); a CADR in excess of the modeled target was consistently achieved with this prototype design. Key field testing results are presented in *Table 1*; for supplemental indoor and outdoor environmental results, see *Table A.3* in the Appendix.

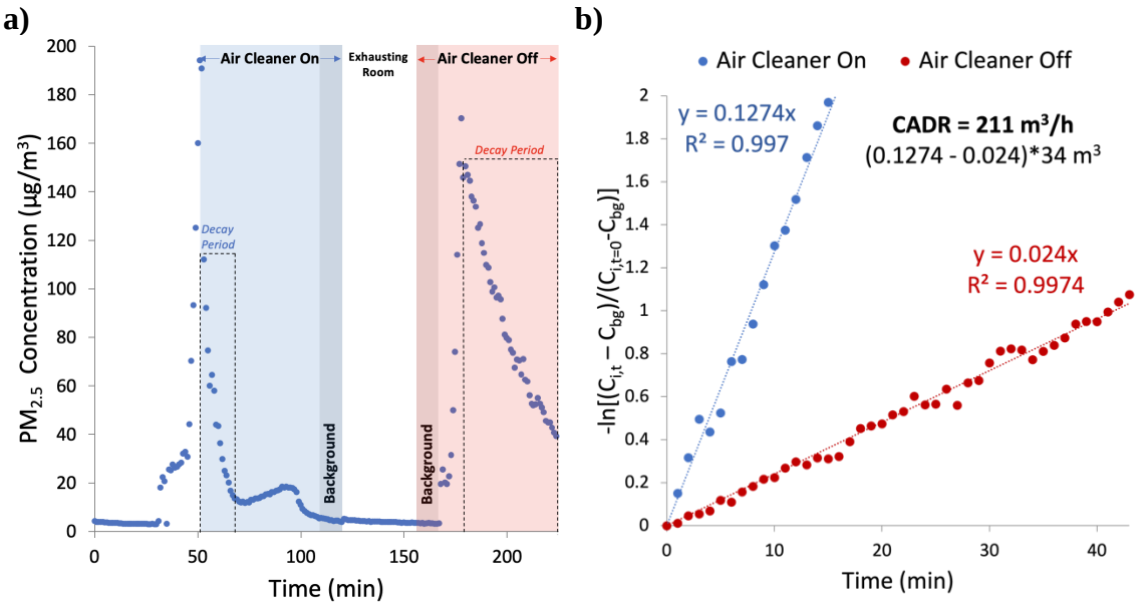

Figure 6: a) $PM_{2.5}$ concentration vs. time plot and *b)* linear regression plot for the air cleaner on and air cleaner off tests at location 1 on 05/02/21; slopes correspond to particle loss rate constants and CADR calculation is shown

Table 1: Key field testing results

	Location 1		**Location 2**	
	Trial 1	*Trial 2*	*Trial 1*	*Trial 2*
CADR (m^3/h)	165	211	157	174
Net $PM_{2.5}$ Reduction After 30 Minutes (%)	85	77	84	88
Air Exchange Rate (h^{-1})	0.77	0.77	0.84	0.84

4.3 Laboratory Testing

4.3.1 Airflows

Figure 7 presents air cleaner flowrates measured using the pressure matching method described in *Section 3.2.2*. Three readings for each of the five fabrics and two MERV 13 filter-based configurations (with and without an airflow-increasing shroud) were averaged over one minute—all air cleaners were powered with the same box fan (Comfort Zone Model CZ200A).

While manufacturer specifications did not provide a maximum air flowrate for the box fan, a review of several common 0.5 m retail box fans found that a maximum flow rate of about 1700 m^3/h is common. Several third-party retailers claim a flowrate of 1087 m^3/h for the model we used, but do not report the associated fan speed setting; this flowrate is in agreement with our filterless fan at a low speed. The volume of air that can be passed through the fabric filter depends upon the properties of the material—a thicker, less permeable fabric such as polyester adds static pressure to the system while a thin fabric such as chiffon allows air to pass through it easily. The cotton batting and felt air cleaner configurations produced air flowrates within 10% of each other at each fan speed, which

was expected considering the comparable nature of the material. The modified Corsi-Rosenthal Box's flowrates were nearly double those of the single MERV 13 filter configuration, as the substantially larger surface area of filters in the design allowed for lower pressure drop and greater airflow. The airflow-enhancing cardboard shroud increased flowrates for the MERV 13 filter-based configurations by ~13% at each fan speed. *Table B.1* in the Appendix presents the complete dataset of average air cleaner flowrates.

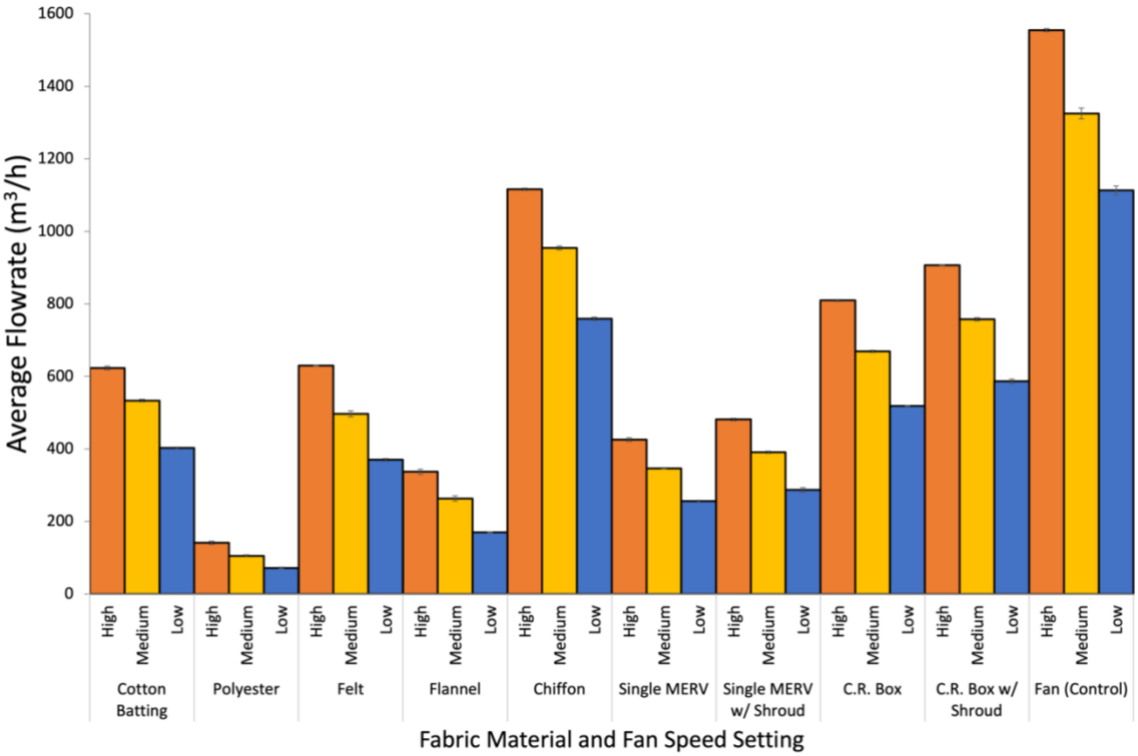

Figure 7: Comparison of average air flowrates (m^3/h) through the air cleaning device

4.3.2 Single-Pass Removal Efficiencies

Removal efficiencies were calculated for five fabrics and a MERV 13 filter across three filter holder diameters (20-, 47-, and 100-mm), which result in three face velocities (0.21, 0.04, and 0.009 m/s) consistent with expectations for the full-scale device. Particle

concentrations were summed and separated into three size bins (0.02–0.3, 0.3–1, and 1–2.5 µm), whose ranges were partially inspired by the size bins presented in the MERV rating section of ANSI/ASHRAE Standard 52.2 (0.3–1, 1–3, and 3–10 µm).[41] We opted to present a range capped at 2.5 µm, as doing so enabled a more straightforward presentation of $PM_{2.5}$ removal efficiency, which is widely used in characterizing the extent of wildfire air pollution. Particles in the 2.5–10 µm range were excluded from this study because the challenge aerosol did not generate a large enough quantity of them to be analyzed with confidence. Though ANSI/ASHRAE Standard 52.2 calls for testing of in-duct filters at a face velocity of 2.5 m/s—which is more than 1000% higher than the largest face velocity realized during this experiment—MERV 13 removal efficiencies were just ~10% less than minimum size-resolved values reported by the standard (85% in the 1–3 µm range and 50% in the 0.3–1 µm range).

Figure 8 displays average removal efficiencies across two trials for the 47 mm diameter filter holder, chosen for presentation here because it is most representative of the diameter of filter holder needed (41 mm) to match the face velocity of the device with a cotton batting filter attached at the high fan speed setting (0.05 m/s). The cotton batting filter proved to have the highest removal efficiency in each size bin—16% at 0.02–0.3 µm, 13% at 0.3–1 µm, and 31% at 1–2.5 µm, respectively—and was thus the presumptive front-runner for large-scale chamber testing. *Table B.2* in the Appendix presents complete results (average ± range) at each of the filter holder diameters.

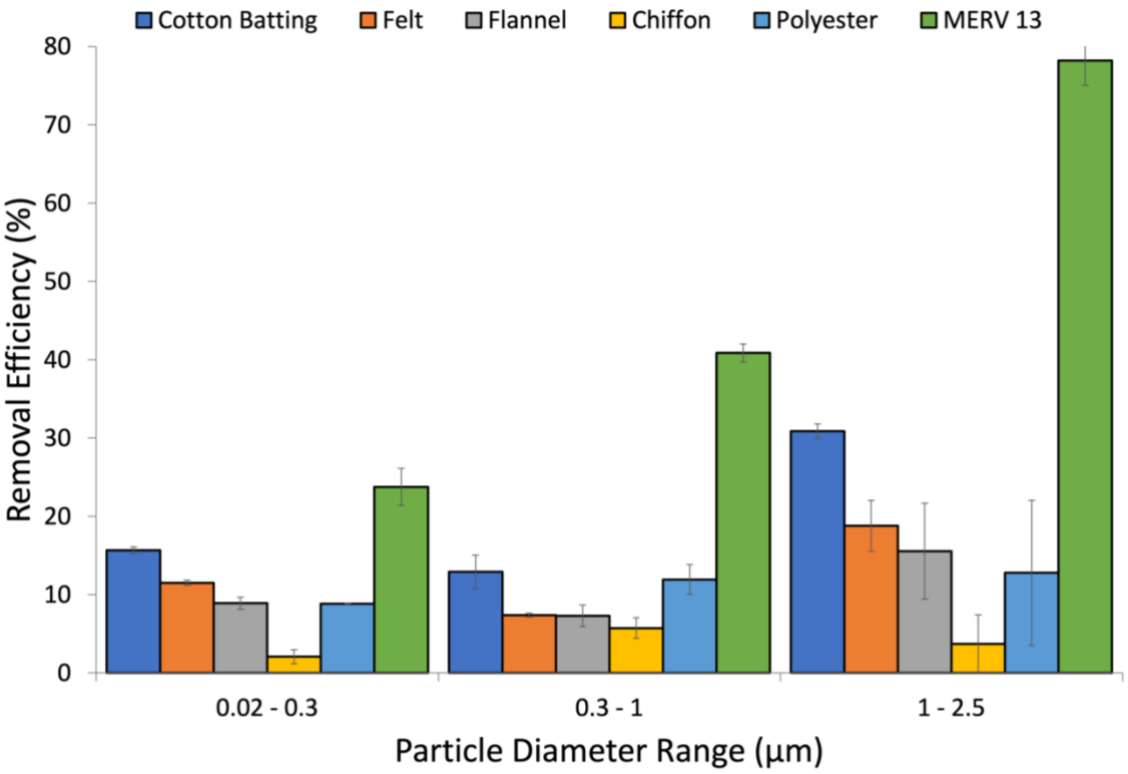

Figure 8: Average removal efficiencies (%) for the 47 mm diameter filter holder

4.3.3 Predicted CADRs from Laboratory Testing

Using *Equation 3*, average predicted CADRs across two trials were calculated for the prototype device with each of the five fabrics attached. For comparison, CADRs were also calculated for four popular, homemade, MERV 13 filter-based air cleaning device configurations, namely a box fan with a single MERV 13 filter attached to it and a modified Corsi-Rosenthal Box comprised of four filters; both were tested with and without flow-increasing shrouds. *Figure 9* presents a comparison of average predicted CADRs across three particle size bins for trials executed with the 47 mm diameter filter holder at the high fan speed setting.

MERV 13 filter-based configurations yielded considerably higher CADRs in comparison to fabric-based configurations, which was expected due to the filter's high

removal efficiency. A single MERV 13 filter affixed to a box fan yielded predicted CADRs of 101 ± 20, 174 ± 10, and 333 ± 27 m^3/h in the 0.02–0.3, 0.3–1, and 1–2.5 µm size bins, respectively. The addition of a shroud increased average predicted CADRs across all size bins by ~12% in the case of the single MERV 13 filter and ~13% in the case of the Corsi-Rosenthal Box. The latter of the two DIY configurations is designed in the shape of a cube, so that in addition to the high removal efficiencies realized by the MERV 13 filter, airflow is less restricted. The Corsi-Rosenthal Box with airflow-increasing shroud produced the highest average predicted CADRs of the experiment: 215 ± 43, 371 ± 21, and 709 ± 57 m^3/h in the 0.02–0.3, 0.3–1, and 1–2.5 µm size bins, respectively.

Comparing these results to those present in the literature, for a single MERV 13 filter affixed to a box fan and Corsi-Rosenthal box (both tested at their highest fan speeds), Holder et al. 2022[1] determined $PM_{2.5}$ CADRs of 189 ± 2 m^3/h and 681 ± 52 m^3/h, respectively. Adding a shroud to the MERV 13 filter affixed to a box fan caused the CADR to increase by 29% to 265 ± 6 m^3/h. There was general agreement between their results and the predicted CADRs of this study despite differences in methodology and materials. Holder et al. 2022[1] followed the ANSI/AHAM AC-1 test method described in *Section 2.3* more closely than we did, using a mixture of flaming and smoldering pine needles as the challenge aerosol and determining CADRs from pull-down results in a large chamber. While this process is similar to the large-scale chamber testing method we employed (described in *Section 3.2.4*), for this phase of experiments, we chose to predict CADRs by combining air flowrates and single-pass removal efficiencies.

Dal Porto et al. 2022[35] determined $PM_{2.5}$ CADRs as high as 1450 m^3/h when testing the Corsi-Rosenthal box at its highest fan speed setting. While this CADR is significantly larger than the predicted CADRs found as part of this experiment, the discrepancy between results could be explained by their use of a different challenge aerosol (NaCl), five MERV 13 filters instead of four, and an Aerodynamic Particle Sizer (APS 3321) to measure particulate matter, which records particle diameters from 0.5–20 µm.

Using the pull-down method in a large chamber, Zeng et al. 2021[42] tested a five-panel, MERV 13 filter-based Corsi-Rosenthal box (equipped with an air flowrate-increasing shroud) at its highest fan speed with burning incense and vacuum cleaner dust as the challenge aerosols; they reported CADRs of 263, 442, and 545 m^3/h in 0.01–0.4, 0.3–1, and 0.5–3 µm particle diameter ranges, respectively. Analyzing these results against the average predicted CADRs we determined for the Corsi-Rosenthal box with flowrate-increasing shroud, there is an 18%, 16%, and 30% difference when comparing CADRs in the 0.02–0.3, 0.3–1, and 1–2.5 µm diameter range to the 0.01–0.4, 0.3–1, and 0.5–3 µm ranges reported in their study. Despite differing test methods, challenge aerosols, instrumentation, and filter surface areas, our results were in relatively close agreement.

Again, of the fabric configurations, the device with a cotton batting filter attached proved to have the highest CADR in each size bin—98 m^3/h at 0.02–0.3 µm, 80 m^3/h at 0.3–1 µm, and 192 m^3/h at 1–2.5 µm, respectively—and was thus the configuration chosen for large-scale chamber testing. *Table B.3* in the Appendix presents size-resolved predicted CADRs (average ± range) for the five fabric and four MERV 13 filter-based configurations at each of the filter holder diameters.

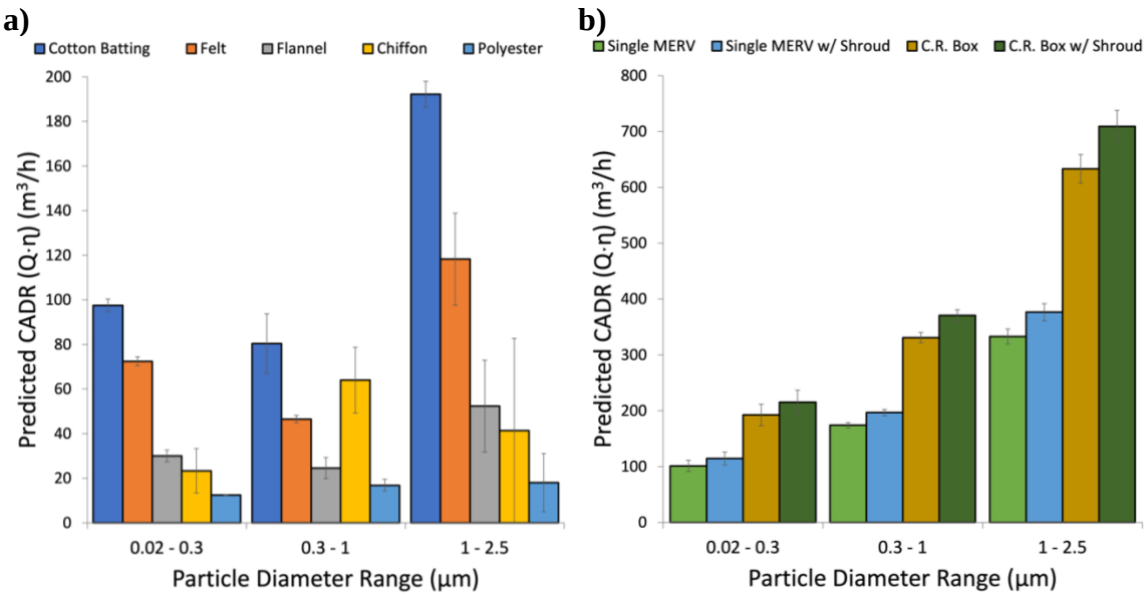

Figure 9: Average predicted CADRs (m^3/h) for *a)* fabric filter configurations and *b)* MERV 13 filter configurations. All predicted CADRs are from trials with a 47 mm diameter filter holder at the high fan speed setting.

4.4 Large-Scale Chamber Testing

Triplicate experiments were conducted for the air cleaning device with a single cotton batting fabric filter attached, a double layer of cotton batting fabric filter attached, and a double layer of cotton batting fabric filter attached with a flow-increasing shroud affixed to the outtake side of the box fan. *Figure 10* presents $PM_{2.5}$ concentrations over the course of a representative experiment where the double layer of cotton batting fabric was tested. As expected, concentrations decrease more rapidly during the portion of the experiment where the air cleaner is engaged versus when it is not. Note that these results look similar to those presented in *Figure 6a*, but the experiment is being carried out in a better controlled environment with more sophisticated particle counting equipment.

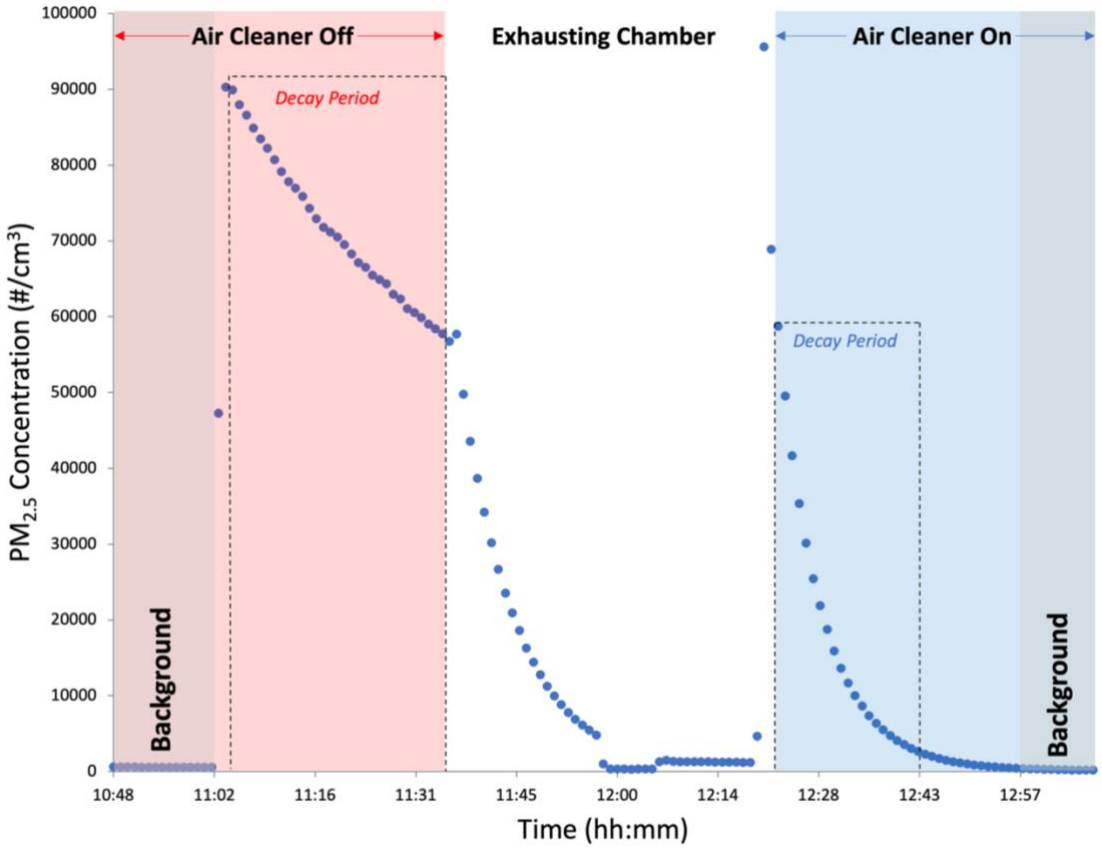

Figure 10: $PM_{2.5}$ concentration (particles/cm^3) vs. time for trial 2 of the double fabric chamber experiment

Table 2 presents average CADRs (m^3/h), separated by particle diameter range, for the three configurations of the air cleaner tested. The air cleaner with two layers of cotton batting filter and an airflow-increasing shroud attached proved to have the highest CADR across all particle size ranges. Adding a second layer of fabric increased CADRs by 40%, 50%, and 7% in the 0.02–0.3, 0.3–1, and 1–2.5 µm particle diameter ranges; additional filter surface area likely increased the removal efficiency of the device. The addition of a flowrate-increasing shroud to the double fabric configuration, however, only increased CADRs by 4%, 1%, and 11% in the 0.02–0.3, 0.3–1, and 1–2.5 µm particle diameter ranges. *Table C.1* in the Appendix presents size-resolved CADRs and particulate matter

loss rates (average ± standard deviation), as well as supplemental environmental information.

Table 2: Large-scale chamber testing CADR averages and standard deviations (m^3/h)

	0.02–0.3 µm	*0.3–1 µm*	*1–2.5 µm*
Single Fabric	131 ± 9	104 ± 9	204 ± 16
Double Fabric	183 ± 5	156 ± 7	218 ± 51
Double Fabric w/ Shroud	190 ± 12	158 ± 7	243 ± 69

4.5 Comparison of Experiments

The purpose of this study was to experimentally determine and improve the CADR of low-cost, DIY air cleaning devices using various methods. Several configurations of the device were tested during each experimental setup—with variables such as type of fabric, fan speed, etc. being altered—making a direct comparison between results difficult. Focusing on the two highly controlled experiments (laboratory and large-scale chamber testing), an additional round of experimentation was conducted to make such a comparison possible. Using the large-scale chamber testing method described in *Section 3.2.4*, triplicate experiments were performed on a configuration of the device that included the box fan used during laboratory testing operated at its highest setting and a single cotton batting filter, with incense burnt on a hot plate as the challenge aerosol. *Figure 11* compares the average CADRs of the laboratory and large-scale chamber studies across three particle diameter ranges.

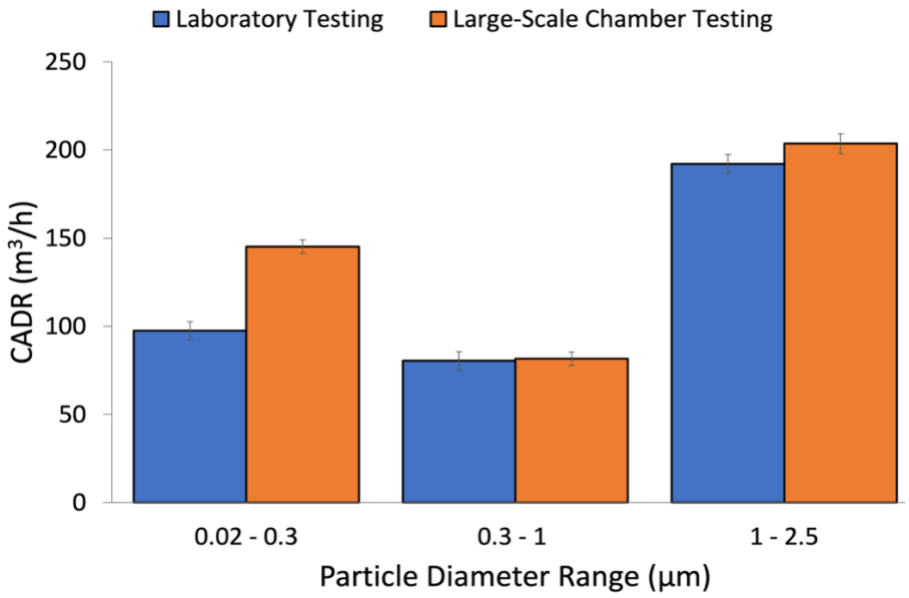

Figure 11: Comparison of laboratory and large-scale chamber testing CADRs (m^3/h) for a single layer of cotton batting fabric at the highest fan speed setting with incense as the challenge aerosol

The device yielded average CADRs that were 49%, 1%, and 6% higher than the corresponding laboratory experiment predicted CADRs, at particle size ranges of 0.02–0.3, 0.3–1, and 1–2.5 µm, respectively. While laboratory testing underpredicted CADRs in the 0.02–0.3 µm size range, there was agreement between the two experimental approaches in the two larger size bins that were analyzed.

This discrepancy in the smaller size bin could potentially be attributed to different particulate matter loss mechanisms occurring within the two enclosures. During the large-scale chamber testing described in this section, relative humidity was recorded at 28 ± 1% for periods when the air cleaner was operational, which is lower than the range deemed acceptable (40 ± 5%) by the ANSI/AHAM AC-1 test method outlined in *Section 2.3*. Though relative humidity was not monitored during laboratory testing, the same run of well-sealed ducting was used to expose glass and cotton samples to pine needle combustion emissions shortly after the conclusion of our experimental campaign. Relative humidity

was recorded during eight hour exposure periods, beginning at approximately 60%, peaking just below 75%, and decreasing to about 55% during the first hour following injection. Because increased relative humidity causes particulate matter to grow in size,[43] particles near the lower end of the 0.02–0.3 μm diameter range may have developed into larger particles on the higher end of the same range; Li et al. 2015[44] observed this phenomenon while analyzing the size distribution of smoke from burning biomass. Plotting particle diameter as a function of removal efficiency for MERV filters, a trend emerges where efficiency steadily decreases from 0.01 μm to ~0.2 μm, after which it increases until ~3 μm.[45] Li et al. 2015[44] found that combustion processes generate particles in the 0.02–0.05 μm size range; if small particles were growing due to elevated relative humidity but remaining less than 0.3 μm in diameter, the increased difficulty with which they were able to be removed would reduce CADRs in the 0.02–0.3 μm size bin.

During the single-pass removal efficiency experiments described in *Section 3.2.3,* $PM_{2.5}$ concentrations reached an average peak of ~19,000 particles/cm^3 across the two 47 mm cotton batting trials. In comparison, average peak $PM_{2.5}$ concentrations of ~100,000 particles/cm^3 were reached across the final three large-scale chamber experiments, a 426% increase. Particle concentrations were more difficult to control during these final chamber trials, as extinguishing the burning incense required entering the chamber and manually disengaging the hot plate. The time it took for the burning incense to elevate particulate matter levels was highly variable, and a delay in the on-screen particle counter readings used to determine when target peak concentrations were reached caused a consistent exceeding of the intended $PM_{2.5}$ threshold.

With MERV 13 filter-based designs that yielded CADRs greater than 340 m^3/h, Holder et al. 2022[1] found a linearly increasing relationship between CADR and initial $PM_{2.5}$ concentration. Acknowledging that concentration levels are not expected to have an effect on CADR,[46] the authors of the study propose that a shift to larger particle sizes occurs at higher concentrations; larger particles can be removed more efficiently by MERV 13 filters.[45] Though the filter tested here was constructed of cotton batting, this trend suggests that because peak $PM_{2.5}$ concentrations were higher during large-scale chamber experiments, particles were removed from the 0.02–0.3 μm size bin due to agglomeration, growing into the 0.3–1 μm size bin. Agglomeration is a removal mechanism that we were unable to control for, especially as we transitioned from a smaller enclosure to a larger one (the run of ducting was 0.5 m^3 while the chamber was 21 m^3) and reached different peak concentrations during particulate matter injections. This phenomenon would leave less particulate matter to remove in the 0.02–0.3 μm size bin and could explain a higher CADR during chamber experiments. Additionally, exposing the cotton batting filter (which is woven relatively loosely) to higher $PM_{2.5}$ concentrations may have loaded it more quickly, thus increasing its short-term particle removal effectiveness. Future experiments will include a Scanning Mobility Particle Sizer (TSI, Model 3910), which measures nanoparticles in the 10–420 nm range, to further explore this discrepancy in the 0.02–0.3 μm size bin.

Section 5: Conclusion

In this study, we evaluated a range of low-cost, DIY air cleaner designs that may reduce exposures to indoor particulate matter. In addition to characterizing box fan-based air cleaners that rely on high MERV-rated filters, we characterized a novel alternative design where a simple fabric filter is used in place of a traditional mechanical filter. This alternative addresses several challenges, chiefly the limited availability of high MERV-rated filters in affected areas during wildfire events. The filter-based designs presented here are constructed from low-cost, sustainable materials that would be accessible to most during such an event.

Air cleaners and filter materials were tested using three distinct methods: 1) field testing, where particle decay tests in two residential homes were conducted on the device, 2) laboratory testing, where air flowrates and filter single-pass removal efficiencies were tested independently and combined to calculate a predicted CADR, and 3) large-scale chamber testing, which employed particle decay testing inside of a well-sealed chamber. While, as expected, MERV filter-based devices yielded higher CADRs, the fabric-based design with a cotton batting filter attached proved to be effective in reducing $PM_{2.5}$ concentrations. Testing results indicate that CADRs can be achieved that meet common air-cleaner sizing requirements for small rooms.[31]

During the field study, the prototype equipped with a cotton batting filter had a net $PM_{2.5}$ removal effectiveness of >80% within 30 minutes of operation and yielded CADRs in excess of 170 m^3/h. At the highest fan speed setting with a single layer of fabric, average predicted CADRs of 98 m^3/h in the 0.02–0.3 µm size bin, 80 m^3/h in the 0.3–1 µm size

bin, and 192 m^3/h in the 1–2.5 μm size bin were realized during laboratory testing. At the highest fan speed setting with a double layer of fabric and flow-increasing shroud, average CADRs of 190 m^3/h in the 0.02–0.3 μm size bin, 158 m^3/h in the 0.3–1 μm size bin, and 243 m^3/h in the 1–2.5 μm size bin were realized. An additional round of large-scale chamber tests designed to directly compare results across experimental setups showed that the device yielded average CADRs that were 49%, 1%, and 6% higher than the corresponding laboratory experiment predicted CADRs, at particle size ranges of 0.02–0.3, 0.3–1, and 1–2.5 μm, respectively. While there was agreement between these experimental approaches in the two larger size bins, laboratory testing underpredicted CADRs in the 0.02–0.3 μm size range, a discrepancy that could be explained by relative humidity and peak $PM_{2.5}$ injection concentration inconsistencies across experiments.

Working with interested parties in Portland, Oregon, we intend to manufacture inexpensive fabric-based air-cleaning kits for emergency use. Additionally, we are in the process of drawing up an instructional document that outlines methods for producing configurations of the device based on what items are available to the person in need. From the beginning, our research has been motivated by a desire to assist the community; all emergency kits will be sold at cost and instructional documents will be distributed free of charge.

Fabric-based, do-it-yourself air cleaners may represent a viable option for improving indoor air quality during a wildfire event.

References

1. Holder, A. L., Halliday, H. S. & Virtaranta, L. Impact of do-it-yourself air cleaner design on the reduction of simulated wildfire smoke in a controlled chamber environment. *Indoor Air* **32**, e13163 (2022).
2. Stauffer, D. A., Autenrieth, D. A., Hart, J. F. & Capoccia, S. Control of wildfire-sourced PM2.5 in an office setting using a commercially available portable air cleaner. *Journal of Occupational and Environmental Hygiene* **17**, 109–120 (2020).
3. Henderson, D. E., Milford, J. B. & Miller, S. L. Prescribed Burns and Wildfires in Colorado: Impacts of Mitigation Measures on Indoor Air Particulate Matter. *Journal of the Air & Waste Management Association* **55**, 1516–26 (2005).
4. Environmental Protection Agency. Air Quality | National Summary | US EPA. *Air Quality Trends* https://www.epa.gov/air-trends/air-quality-national-summary (2020).
5. Hoover, K. & Hanson, L. A. Wildfire Statistics. *Congressional Research Service* (2018).
6. Abatzoglou, J. T. & Williams, A. P. Impact of anthropogenic climate change on wildfire across western US forests. *Proceedings of the National Academy of Sciences* **113**, 11770–11775 (2016).
7. Liu, J. C. *et al.* Wildfire-specific Fine Particulate Matter and Risk of Hospital Admissions in Urban and Rural Counties. *Epidemiology* **28**, 77–85 (2017).
8. Reid, C. E. *et al.* Critical Review of Health Impacts of Wildfire Smoke Exposure. *Environmental Health Perspectives* **124**, 1334–1343 (2016).
9. Reid, C. E. & Maestas, M. M. Wildfire smoke exposure under climate change: impact on respiratory health of affected communities. *Curr Opin Pulm Med* **25**, 179–187 (2019).
10. Chen, H., Samet, J. M., Bromberg, P. A. & Tong, H. Cardiovascular health impacts of wildfire smoke exposure. *Part Fibre Toxicol* **18**, 2 (2021).
11. Liu, J. C., Pereira, G., Uhl, S. A., Bravo, M. A. & Bell, M. L. A systematic review of the physical health impacts from non-occupational exposure to wildfire smoke. *Environmental Research* **136**, 120–132 (2015).
12. Holm, S. M., Miller, M. D. & Balmes, J. R. Health effects of wildfire smoke in children and public health tools: a narrative review. *J Expo Sci Environ Epidemiol* **31**, 1–20 (2021).
13. Henry, S., Ospina, M. B., Dennett, L. & Hicks, A. Assessing the Risk of Respiratory-Related Healthcare Visits Associated with Wildfire Smoke Exposure in Children 0–18 Years Old: A Systematic Review. *International Journal of Environmental Research and Public Health* **18**, 8799 (2021).
14. Liu, J. C. *et al.* Who Among the Elderly Is Most Vulnerable to Exposure to and Health Risks of Fine Particulate Matter From Wildfire Smoke? *American Journal of Epidemiology* **186**, 730–735 (2017).
15. Park, B. R., Eom, Y. S., Choi, D. H. & Kang, D. H. Estimation of Outdoor PM2.5 Infiltration into Multifamily Homes Depending on Building Characteristics Using Regression Models. *Sustainability* **13**, 5708 (2021).

16. Xu, C. *et al.* Investigation and modeling of the residential infiltration of fine particulate matter in Beijing, China. *Journal of the Air & Waste Management Association* **67**, 694–701 (2017).
17. United States Environmental Protection Agency Indoor Environmental Division. *Residential air cleaners: a summary of available information.* (USEnvironmental Protection Agency, Office of Air and Radiation, Indoor Environments Division, 2009).
18. US EPA, O. Cleaner Indoor Air During Wildfires Challenge. https://www.epa.gov/air-research/cleaner-indoor-air-during-wildfires-challenge (2020).
19. Berardi, B. M., Leonie, E., Marchesini, B., Cascella, D. & Raffi, G. B. Indoor climate and air quality in new offices: effects of a reduced air-exchange rate. *Int. Arch Occup Environ Heath* **63**, 233–239 (1991).
20. Murray, D. M. & Burmaster, D. E. Residential Air Exchange Rates in the United States: Empirical and Estimated Parametric Distributions by Season and Climatic Region. *Risk Analysis* **15**, 459–465 (1995).
21. Long, C. M., Suh, H. H., Catalano, P. J. & Koutrakis, P. Using Time- and Size-Resolved Particulate Data To Quantify Indoor Penetration and Deposition Behavior. *Environmental science & technology* **35**, 2089–2099 (2001).
22. Kim, K.-H., Pandey, S. K., Kabir, E., Susaya, J. & Brown, R. J. C. The modern paradox of unregulated cooking activities and indoor air quality. *Journal of Hazardous Materials* **195**, 1–10 (2011).
23. Liao, C.-M. *et al.* Lung cancer risk in relation to traffic-related nano/ultrafine particle-bound PAHs exposure: A preliminary probabilistic assessment. *Journal of Hazardous Materials* **190**, 150–158 (2011).
24. Arashidani, K. *et al.* Indoor Pollution from Heating. *Industrial health* **34**, 205–215 (1996).
25. Nazaroff, W. W. & Weschler, C. J. Cleaning products and air fresheners: exposure to primary and secondary air pollutants. *Atmospheric Environment* **38**, 2841–2865 (2004).
26. Halios, C. H., Assimakopoulos, V. D., Helmis, C. G. & Flocas, H. A. Investigating cigarette-smoke indoor pollution in a controlled environment. *Science of The Total Environment* **337**, 183–190 (2005).
27. Missia, D. A., Demetriou, E., Michael, N., Tolis, E. I. & Bartzis, J. G. Indoor exposure from building materials: A field study. *Atmospheric Environment* **44**, 4388–4395 (2010).
28. Haghighat, F. & Donnini, G. Emissions of Indoor Pollutants from Building Materials—State of the Art Review. *Architectural Science Review* **36**, 13–22 (1993).
29. Thatcher, T. L., Lai, A. C. K., Moreno-Jackson, R., Sextro, R. G. & Nazaroff, W. W. Effects of room furnishings and air speed on particle deposition rates indoors. *Atmospheric Environment* **36**, 1811–1819 (2002).
30. ASHRAE Position Document on Filtration and Air Cleaning. (2021).

31. ANSI/AHAM AC-1-2015 - Method for Measuring Performance of Portable Household Electric Room Air Cleaners. https://webstore.ansi.org/standards/aham/ansiahamac2015.
32. Xiang, J. *et al.* Field measurements of PM2.5 infiltration factor and portable air cleaner effectiveness during wildfire episodes in US residences. *Science of The Total Environment* **773**, 145642 (2021).
33. He, J. *et al.* Network of low-cost air quality sensors for monitoring indoor, outdoor, and personal PM2.5 exposure in Seattle during the 2020 wildfire season. *Atmospheric Environment* **285**, 119244 (2022).
34. May, N. W., Dixon, C. & Jaffe, D. A. Impact of Wildfire Smoke Events on Indoor Air Quality and Evaluation of a Low-cost Filtration Method. *Aerosol Air Qual. Res.* **21**, 210046 (2021).
35. Dal Porto, R., Kunz, M. N., Pistochini, T., Corsi, R. L. & Cappa, C. D. Characterizing the performance of a do-it-yourself (DIY) box fan air filter. *Aerosol Science and Technology* **56**, 564–572 (2022).
36. Steinle, S. *et al.* Personal exposure monitoring of PM2.5 in indoor and outdoor microenvironments. *Science of The Total Environment* **508**, 383–394 (2015).
37. Rice, A. & Bostrom, G. Measurements of carbon dioxide in an Oregon metropolitan region. *Atmospheric Environment* **45**, 1138–1144 (2011).
38. Drewnick, F. *et al.* Aerosol filtration efficiency of household materials for homemade face masks: Influence of material properties, particle size, particle electrical charge, face velocity, and leaks. *Aerosol Science and Technology* **55**, 63–79 (2021).
39. Minneapolis Duct Blaster Operation Manual. (2011).
40. Chen, W., Zhang, J. & Zhang, Z. B. Performance of Air Cleaners for Removing Multi-Volatile Organic Compounds in Indoor Air. *ASHRAE Transactions* **111**, 1101–1114 (2005).
41. ANSI/ASHRAE Standard 52.2-2017.
42. Zeng, Yicheng, Heidarinejad, Mohammad, & Stephens, Brent. Portable Air Cleaner Test Report: 'Corsi-Rosenthal' Box Fan Air Cleaner w/ MERV 13 Filters. https://www.built-envi.com/wp-content/uploads/IIT-CADR-Testing-C-R-Box-September-2021.pdf (2021).
43. Han, J., Liu, X., Chen, D. & Jiang, M. Influence of relative humidity on real-time measurements of particulate matter concentration via light scattering. *Journal of Aerosol Science* **139**, 105462 (2020).
44. Li, C. *et al.* Evolution of biomass burning smoke particles in the dark. *Atmospheric Environment* **120**, 244–252 (2015).
45. Dols, W., Polidoro, B., Poppendieck, D. & Emmerich, S. *A Tool to Model the Fate and Transport of Indoor Microbiological Aerosols (FaTIMA)*. (2020). doi:10.6028/NIST.TN.2095.
46. Zhang, Y. *et al.* Can commonly-used fan-driven air cleaning technologies improve indoor air quality? A literature review. *Atmospheric Environment* **45**, 4329–4343 (2011).

Appendix A: Field Testing

A.1: Field Testing Images

a) **b)**

Figure A.1: Images of the experimental setup at *a)* location 1 and *b)* location 2

A.2: Air Exchange Rates

a) **b)**

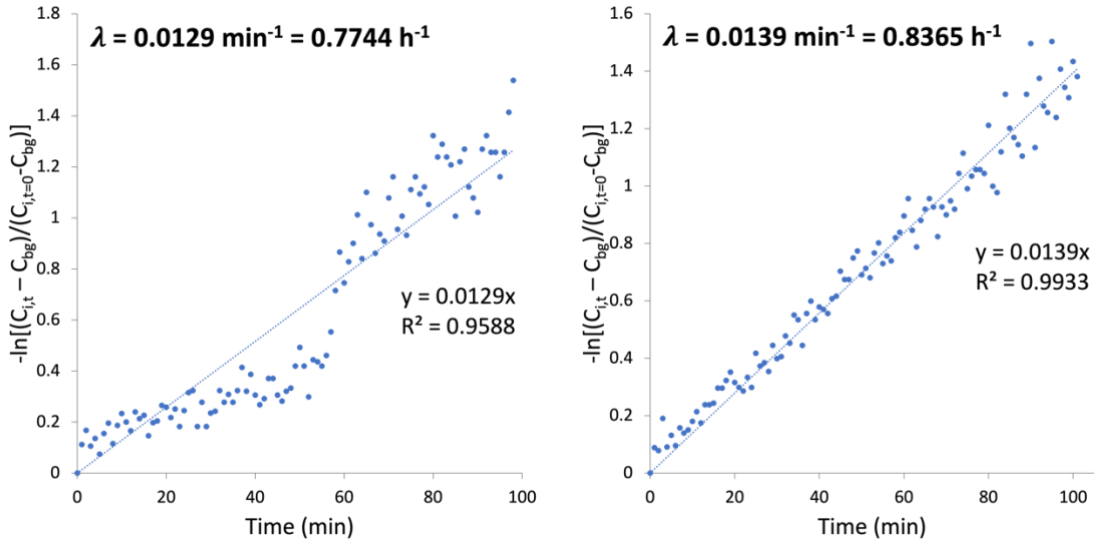

Figure A.2: Air exchange rates as determined by a CO_2 tracer decay test at locations *a)*1 and *b)* 2. Regression analysis is shown. Slopes correspond to air exchange rates: 0.77 h^{-1} at location 1 and 0.84 h^{-1} at location 2.

A.3: Field Testing Results

Table A.3: Supplemental and environmental field testing results over the course of four days in two separate locations (described in *Section 3.2.1*).

	Location 1		**Location 2**	
	Trial 1	*Trial 2*	*Trial 1*	*Trial 2*
Date	05/01/21	05/02/21	04/22/21–04/23/21	04/23/21
Time	14:20–18:36	11:02–14:35	21:29–0:37	8:58–11:07
Room Volume (m^3)	34	34	582.06	582.06
Sound Level (dB)	45	45	16.5	16.5
Indoor Temperature (°C)	19.5	20.2	18.3	13.5
Outdoor Temperature (°C)	24	13	18	16
Indoor Relative Humidity (%)	51	48	42	48
Outdoor Humidity (%)	36	52	57	63
Outdoor Wind Speed (m/s)	2.2	1.8	3.6	2.7
Outdoor Average $PM_{2.5}$ Concentration ($\mu g/m^3$)	1.0	1.8	5.8	7.6
Air Exchange Rate (h^{-1})	0.77	0.77	0.84	0.84
$PM_{2.5}$ Loss Rate (Air Cleaner Off) (h^{-1})	0.51	1.44	2.30	2.63
$PM_{2.5}$ Loss Rate (Air Cleaner On) (h^{-1})	5.37	7.64	11.803	13.18
CADR (m^3/h)	165	211	157	174
Net $PM_{2.5}$ Reduction After 30 Min. (%)	85	77	84	88

Appendix B: Laboratory Testing

B.1: Airflows

Table B.1: Air cleaner flowrates (average +/- standard deviation) for five fabrics and two MERV 13 filter configurations, with and without a shroud. Three readings for each configuration were averaged over one minute.

Material	**Low Speed (m^3/h)**	**Medium Speed (m^3/h)**	**High Speed (m^3/h)**
Cotton Batting	403 ± 3	533 ± 3	623 ± 5
Polyester	72 ± 3	105 ± 3	141 ± 4
Felt	370 ± 3	497 ± 9	630 ± 1
Flannel	170 ± 2	263 ± 7	337 ± 7
Chiffon	759 ± 5	954 ± 5	1116 ± 3
Single MERV 13	256 ± 3	347 ± 2	426 ± 5
Single MERV 13 w/ Shroud	287 ± 3	391 ± 3	481 ± 4
C.R. Box	519 ± 1	669 ± 3	810 ± 3
C.R. Box w/ Shroud	587 ± 6	758 ± 4	907 ± 1
Fan (Control)	1113 ± 13	1325 ± 15	1555 ± 4

B.2: Single-Pass Removal Efficiencies

Table B.2: Size-resolved (0.02–0.3, 0.3–1, and 1–2.5 µm) single-pass removal efficiencies (average ± range in %) for five fabrics (cotton batting, felt, flannel, chiffon, and polyester) and a MERV 13 filter. Duplicate experiments were performed at three filter hold diameters (20-, 47-, and 100-mm).

		Single-Pass Removal Efficiency (%)					
Filter Holder Diameter (mm)	**Particle Diameter Range (µm)**	*Cotton Batting*	*Felt*	*Flannel*	*Chiffon*	*Polyester*	*MERV 13*
20	*0.02–0.3*	10.4 ± 0.5	12.0 ± 3.1	5.4 ± 6.5	1.6 ± 1.2	6.7 ± 0.5	20.0 ± 6.4
	0.3–1	9.1 ± 2.1	6.4 ± 2.2	9.4 ± 4.5	0.1 ± 2.6	10.1 ± 5.9	32.8 ± 1.9
	1–2.5	21.7 ± 1.7	14.4 ± 6.7	16.3 ± 26.4	0.1 ± 23.1	23.7 ± 11.2	65.9 ± 9.8
47	*0.02–0.3*	15.7 ± 0.9	11.5 ± 0.6	8.9 ± 1.5	0.0 ± 1.8	8.8 ± 0.0	23.8 ± 4.8
	0.3–1	12.9 ± 4.3	7.4 ± 0.5	7.3 ± 2.8	0.1 ± 2.6	11.9 ± 3.8	40.9 ± 2.3
	1–2.5	30.9 ± 1.9	18.8 ± 6.6	15.5 ± 12.2	0.0 ± 7.4	12.8 ± 18.5	78.2 ± 6.3
100	*0.02–0.3*	38.9 ± 0.8	30.1 ± 3.8	26.0 ± 14.4	0.0 ± 1.9	13.0 ± 1.7	60.5 ± 10.2
	0.3–1	29.8 ± 2.4	15.5 ± 6.3	18.3 ± 4.1	0.0 ± 0.7	15.1 ± 7.4	79.5 ± 0.8
	1–2.5	74.0 ± 3.5	44.5 ± 30.0	40.1 ± 14.3	0.1 ± 7.9	43.7 ± 3.9	93.7 ± 5.8

B.3: Predicted CADRs

Table B.3: Size-resolved (0.02–0.3, 0.3–1, and 1–2.5 µm) predicted CADRs (average ± range in m^3/h) for five fabric configurations (cotton batting, felt, flannel, chiffon, and polyester) and four MERV 13 filter-based configurations. Duplicate experiments were performed at three filter hold diameters (20-, 47-, and 100-mm).

		20 mm Filter Holder Diameter			***47 mm Filter Holder Diameter***			***100 mm Filter Holder Diameter***		
Material	**Fan Setting**	*0.02–0.3 µm*	*0.3–1 µm*	*1–2.5 µm*	*0.02–0.3 µm*	*0.3–1 µm*	*1–2.5 µm*	*0.02–0.3 µm*	*0.3–1 µm*	*1–2.5 µm*
Cotton Batting	*High*	65 ± 3	57 ± 13	135 ± 11	98 ± 6	80 ± 27	192 ± 12	243 ± 5	186 ± 15	461 ± 22
	Medium	55 ± 3	49 ± 11	116 ± 9	84 ± 5	69 ± 23	165 ± 10	208 ± 4	159 ± 13	395 ± 19
	Low	42 ± 2	37 ± 9	87 ± 7	63 ± 4	52 ± 17	124 ± 8	157 ± 3	120 ± 10	298 ± 14
Polyester	*High*	9 ± 1	14 ± 8	33 ± 16	12 ± 0	17 ± 5	18 ± 26	18 ± 2	21 ± 10	62 ± 6
	Medium	7 ± 1	11 ± 6	25 ± 12	9 ± 0	13 ± 4	13 ± 20	14 ± 2	16 ± 8	46 ± 4
	Low	5 ± 0	7 ± 4	17 ± 8	6 ± 0	9 ± 3	9 ± 13	9 ± 1	11 ± 5	31 ± 3
Felt	*High*	76 ± 20	40 ± 14	90 ± 42	72 ± 4	46 ± 3	118 ± 41	190 ± 24	98 ± 39	280 ± 189
	Medium	60 ± 16	32 ± 11	71 ± 33	57 ± 3	37 ± 3	93 ± 33	150 ± 19	77 ± 31	221 ± 149
	Low	44 ± 12	24 ± 8	53 ± 25	43 ± 2	27 ± 2	70 ± 24	112 ± 14	58 ± 23	165 ± 111
Flannel	*High*	18 ± 22	32 ± 15	55 ± 89	30 ± 5	25 ± 9	52 ± 41	88 ± 49	62 ± 14	135 ± 48
	Medium	14 ± 17	25 ± 12	43 ± 70	23 ± 4	19 ± 7	41 ± 32	68 ± 38	48 ± 11	106 ± 38
	Low	9 ± 11	16 ± 8	28 ± 45	15 ± 3	12 ± 5	26 ± 21	44 ± 25	31 ± 7	68 ± 24
Chiffon	*High*	18 ± 13	62 ± 29	129 ± 257	23 ± 20	64 ± 29	41 ± 83	12 ± 21	28 ± 8	102 ± 88
	Medium	16 ± 11	53 ± 25	110 ± 220	20 ± 17	55 ± 25	35 ± 71	10 ± 18	24 ± 7	87 ± 75
	Low	12 ± 9	42 ± 20	87 ±175	16 ± 14	44 ± 20	28 ± 56	8 ± 15	19 ± 5	69 ± 60
Single MERV	*High*	85 ± 27	140 ± 8	281 ± 42	101 ± 20	174 ± 10	333 ± 27	258 ± 44	339 ± 3	399 ± 25
	Medium	69 ± 22	114 ± 7	228 ± 34	82 ± 16	142 ± 8	271 ± 22	210 ± 35	276 ± 3	325 ± 20
	Low	57 ± 18	94 ± 5	189 ± 28	68 ± 14	117 ± 7	225 ± 18	174 ± 29	228 ± 2	269 ± 17
Single MERV w/ Shroud	*High*	96 ± 31	158 ± 9	317 ± 47	114 ± 23	197 ± 11	376 ± 30	291 ± 49	383 ± 4	451 ± 28
	Medium	78 ± 25	128 ± 7	258 ± 38	93 ± 19	160 ± 9	306 ± 25	237 ± 40	311 ± 3	366 ± 23
	Low	57 ± 18	94 ± 5	189 ± 28	68 ± 14	117 ± 7	225 ± 18	174 ± 29	228 ± 2	269 ± 17
C.R. Box	*High*	162 ± 51	266 ± 15	534 ± 79	192 ± 38	331 ± 19	633 ± 51	490 ± 83	644 ± 7	759 ± 47
	Medium	134 ± 43	220 ± 13	441 ± 65	159 ± 32	274 ± 15	523 ± 42	405 ± 69	532 ± 5	627 ± 39
	Low	104 ± 33	170 ± 10	342 ± 51	123 ± 25	212 ± 12	406 ± 33	314 ± 53	413 ± 4	486 ± 30
C.R. Box w/ Shroud	*High*	181 ± 58	298 ± 17	598 ± 88	215 ± 43	371 ± 21	709 ± 57	549 ± 93	721 ± 7	849 ± 53
	Medium	151 ± 48	249 ± 14	499 ± 74	180 ± 36	310 ± 17	593 ± 48	459 ± 78	603 ± 6	710 ± 44
	Low	117 ± 37	193 ± 11	387 ± 57	139 ± 28	240 ± 13	459 ± 37	355 ± 60	467 ± 5	550 ± 34

Appendix C: Large-Scale Chamber Testing

C.1: Large-Scale Chamber Testing Results

Table C.1: Size-resolved (0.02–0.3, 0.3–1, 1–2.5, and <2.5 µm) CADRs (m^3/h) and particulate matter loss rates (h^{-1}), air exchange rates (h^{-1}), temperatures (ºC), and relative humidities (%) (average ± standard deviation) for three configurations of the device with cotton batting filter attached. "*Off or On*" refers to whether or not the air cleaner was operational during the given period. "*Inside or Outside*" refers to whether measurements were taken inside the chamber or outside of it (ambient laboratory conditions).

				Air Cleaner Configuration		
	Particle Diameter Range (µm)	*Off or On*	*Inside or Outside*	*Single Fabric*	*Double Fabric*	*Double Fabric w/ Shroud*
CADR (m^3/h)	0.02–0.3			77.19 ± 5.06	107.59 ± 3.22	112.12 ± 7.17
	0.3–1			61.05 ± 5.54	91.91 ± 4.38	92.71 ± 4.11
	1–2.5			120.01 ± 9.47	128.07 ± 30.18	142.84 ± 40.60
	$PM_{2.5}$			76.64 ± 5.01	107.11 ± 2.73	111.16 ± 7.21
Particulate Matter Loss Rate (h^{-1})	0.02–0.3	Off		0.98 ± 0.03	0.81 ± 0.12	0.84 ± 0.03
	0.3–1			0.68 ± 0.14	0.40 ± 0.01	0.52 ± 0.05
	1–2.5			1.51 ± 0.10	1.29 ± 0.11	1.29 ± 0.24
	$PM_{2.5}$			0.97 ± 0.03	0.80 ± 0.12	0.83 ± 0.03
	0.02–0.3	On		7.26 ± 0.38	9.53 ± 0.34	9.88 ± 0.47
	0.3–1			5.65 ± 0.35	7.85 ± 0.37	8.00 ± 0.21
	1–2.5			11.26 ± 0.76	11.66 ± 2.37	12.83 ± 3.11
	$PM_{2.5}$			7.21 ± 0.37	9.47 ± 0.31	9.80 ± 0.47
Air Exchange Rate (h^{-1})		Off		0.15 ± 0.13	0.18 ± 0.02	0.17 ± 0.07
		On		0.19 ± 0.04	0.19 ± 0.04	0.15 ± 0.06
Temperature (ºC)		Off	Inside	26.55 ± 2.03	19.83 ± 0.59	20.38 ± 1.03
		On	Inside	25.25 ± 0.53	20.56 ± 0.60	20.96 ± 0.77
		Off	Outside	18.57 ± 0.52	18.35 ± 0.39	17.87 ± 0.30
		On	Outside	18.59 ± 0.33	18.32 ± 0.58	17.93 ± 0.26
Relative Humidity (%)		Off	Inside	50.68 ± 3.52	65.42 ± 3.39	61.50 ± 2.60
		On	Inside	54.58 ± 1.95	63.28 ± 3.15	60.87 ± 1.69
		Off	Outside	74.97 ± 1.93	68.79 ± 3.58	68.85 ± 1.32
		On	Outside	76.07 ± 3.06	69.21 ± 3.84	68.65 ± 1.28